Journal of
Medicinal Chemistry

Subscriber access provided by Uppsala universitetsbibliotek

Drug Annotation

Discovery of BMS-986235/LAR-1219: A Potent Formyl Peptide Receptor 2 (FPR2) Selective Agonist for the Prevention of Heart Failure

Yoshikazu Asahina, Nicholas R. Wurtz, Kazuto Arakawa, Nancy Carson, Kiyoshi Fujii, Kazunori Fukuchi, Ricardo A. Garcia, Mei-Yin Hsu, Junichi Ishiyama, Bruce Ito, Ellen K Kick, John Lupisella, Shingo Matsushima, Kohei Ohata, Jacek Ostrowski, Yoshifumi Saito, Kosuke Tsuda, Francisco J Villarreal, Hitomi Yamada, Toshikazu Yamaoka, Ruth R. Wexler, David A. Gordon, and Yasuchi Kohno

J. Med. Chem., **Just Accepted Manuscript** • DOI: 10.1021/acs.jmedchem.9b02101 • Publication Date (Web): 14 May 2020

Downloaded from pubs.acs.org on May 15, 2020

Just Accepted

“Just Accepted” manuscripts have been peer-reviewed and accepted for publication. They are posted online prior to technical editing, formatting for publication and author proofing. The American Chemical Society provides “Just Accepted” as a service to the research community to expedite the dissemination of scientific material as soon as possible after acceptance. “Just Accepted” manuscripts appear in full in PDF format accompanied by an HTML abstract. “Just Accepted” manuscripts have been fully peer reviewed, but should not be considered the official version of record. They are citable by the Digital Object Identifier (DOI®). “Just Accepted” is an optional service offered to authors. Therefore, the “Just Accepted” Web site may not include all articles that will be published in the journal. After a manuscript is technically edited and formatted, it will be removed from the “Just Accepted” Web site and published as an ASAP article. Note that technical editing may introduce minor changes to the manuscript text and/or graphics which could affect content, and all legal disclaimers and ethical guidelines that apply to the journal pertain. ACS cannot be held responsible for errors or consequences arising from the use of information contained in these “Just Accepted” manuscripts.

is published by the American Chemical Society. 1155 Sixteenth Street N.W., Washington, DC 20036

Published by American Chemical Society. Copyright © American Chemical Society. However, no copyright claim is made to original U.S. Government works, or works produced by employees of any Commonwealth realm Crown government in the course of their duties.

SCHOLARONE™
Manuscripts

Discovery of BMS-986235/LAR-1219: A Potent Formyl Peptide Receptor 2 (FPR2) Selective Agonist for the Prevention of Heart Failure

Yoshikazu Asahina[*,†], *Nicholas R. Wurtz*[*,‡], *Kazuto Arakawa*[†], *Nancy Carson*[‡], *Kiyoshi Fujii*[†], *Kazunori Fukuchi*[†], *Ricardo Garcia*[‡], *Mei-Yin Hsu*[‡], *Junichi Ishiyama*[†], *Bruce Ito*[#], *Ellen Kick*[‡], *John Lupisella*[‡], *Shingo Matsushima*[†], *Kohei Ohata*[†], *Jacek Ostrowski*[‡], *Yoshifumi Saito*[†], *Kosuke Tsuda*[†], *Francisco Villarreal*[#], *Hitomi Yamada*[†], *Toshikazu Yamaoka*[†], *Ruth Wexler*[‡], *David Gordon*[‡], *Yasushi Kohno*[†].

[†]Discovery Research Laboratories, Kyorin Pharmaceutical Co. Ltd., 2399-1, Nogi, Nogi-Machi, Shimotsuga-Gun, Tochigi, 329-0114, Japan. [‡]Bristol-Myers Squibb Research and Development, P.O. Box 5400, Princeton, New Jersey 08534, United States. [#]Department of Medicine, University of California, San Diego, 9500 Gilman Drive La Jolla, CA 92093.

KEYWORDS: Formyl Peptide Receptor, Resolution of Inflammation, Heart Failure, Conformational Restriction, GPCR Agonist

ABSTRACT: Formyl Peptide Receptor 2 (FPR2) agonists can stimulate resolution of inflammation and may have utility for treatment of diseases caused by chronic inflammation, including heart failure. We report the discovery of a potent and selective FPR2 agonist, and its evaluation in a mouse heart failure model. A simple linear urea with moderate agonist activity served as the starting point for optimization. Introduction of a pyrrolidinone core accessed a rigid conformation that produced potent FPR2 and FPR1 agonists. Optimization of lactam substituents led to the discovery of the FPR2 selective agonist **13c**, BMS-986235/LAR-1219. In cellular assays **13c** inhibited neutrophil chemotaxis and stimulated macrophage phagocytosis, key endpoints to promote resolution of inflammation. Cardiac structure and functional improvements were observed in a mouse heart failure model following treatment with BMS-986235/LAR-1219.

Introduction

Formyl peptide receptors (FPRs) constitute a G-protein coupled chemotactic receptor (GPCR) family, which are mainly expressed in neutrophils and monocytes and play an important role in host defense and inflammation. In humans, three subtypes (FPR1, 2, 3) have been identified.[1–3] FPR1 initiates inflammatory responses such as neutrophil chemotaxis, degranulation, respiratory burst, and cytokine release when activated with ligands such as *N*-formyl-methionyl-leucyl-phenylalanine (fMLF) produced by bacteria.[4] FPR2 is involved in both initiation and resolution of inflammation. FPR2 peptide ligands, such as serum amyloid A (SAA), are associated with production of pro-inflammatory cytokine interleukin (IL)-8,[5] while ligands such as Lipoxin A4 and Annexin A1 have been shown to inhibit migration of neutrophils, differentiate macrophages into pro-wound healing phenotypes and upregulate anti-inflammatory cytokines such as IL-10.[6,7] Thus, FPR2 activates both inflammatory and pro-resolution responses depending on the ligand and its binding regions.[8,9]

Since the first small-molecule FPR agonist was reported in 2004,[10] research groups in academia and industry have reported a diverse set of FPR agonists and antagonists.[11–14] Representative FPR agonists include pyrazolone ureas (Compound 43),[15,16]

benzimidazoles,[17] bridged spiro[2.4]heptanes[18] and aminotriazoles (ACT-389949)[19] (Figure 1). Among these compounds, dual FPR2/FPR1 Compound 43 has been used for proof of concept in vivo studies, including the preservation of cardiac function and prevention of adverse remodeling in rodent heart failure models.[8,16,20] FPR2 agonist ACT-389949 was dosed in Phase 1 clinical trials and induced plasma biomarker changes (e.g. IL-10 and leukocyte levels) in humans after one dose; however, the authors reported tachyphylaxis in the multiday dosing study.[21] Although there are no compounds launched as therapeutic agents to date, FPR2 remains a promising target to resolve chronic inflammation and promote the wound healing processes.

Based on reported FPR biology, we focused on the discovery of FPR2 agonists with pro-resolution activity and selectivity over FPR1. We selected simple urea derivative AG-26 (**1**)[22] as a promising starting point with multiple options for future structural transformation.

Figure 1. Structures of selected reported FPR2 agonists

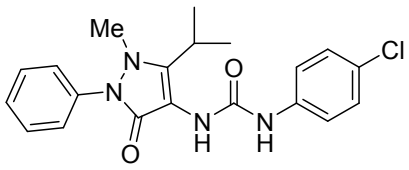

Amgen (2006)
Pyrazolone Urea
(compound 43)

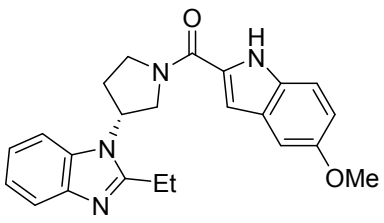

Amgen (2007)
Benzimidazole

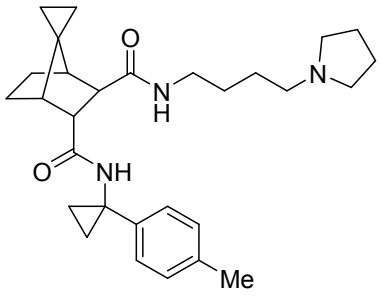

Actelion (2013)
Bridged spiro[2,4]heptane

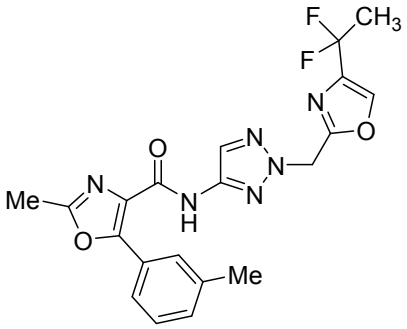

Actelion (2010)
Aminotriazole
(ACT-389949)

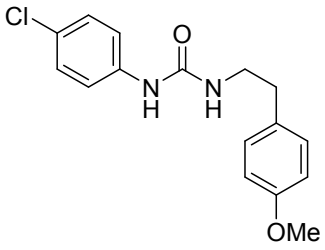

AG-26 (**1**)

Investigation of substituents on the 2-(4-methoxypheny)ethyl moiety of compound **1** resulted in carbamoyl derivative **2d** with enhanced FPR2 activity (Figure 2). In order to investigate conformationally constrained analogs of **2d**, four to six membered lactam derivatives **3**−**7** were prepared. Among these, 5-membered pyrrolidinone derivatives **5** and **6** showed significantly improved activity. Of four optical isomers of **5** and **6**, the (3*S*,4*R*)-form was confirmed to be the most potent FPR2 agonist. Preliminary investigation of the Ar^2 group let to 4-fluorophenyl (3*S*,4*R*) analog **11b**, which exhibited better activity than the 4-chlorophenyl (3*S*,4*R*) analog. Optimization of the Ar^1 group, led

to **12g** bearing the 2,6-difluoro-4-methoxyphenyl group which dramatically improved selectivity over FPR1 without decreasing FPR2 activity. Finally, reoptimization of the Ar^2 group to further improve FPR2 selectivity resulted in the selection of clinical candidate **13c**. Details of this research are described below.

Figure 2. Structure Activity Relationship (SAR) Summary of Pyrrolidinone Urea FPR2 Agonist

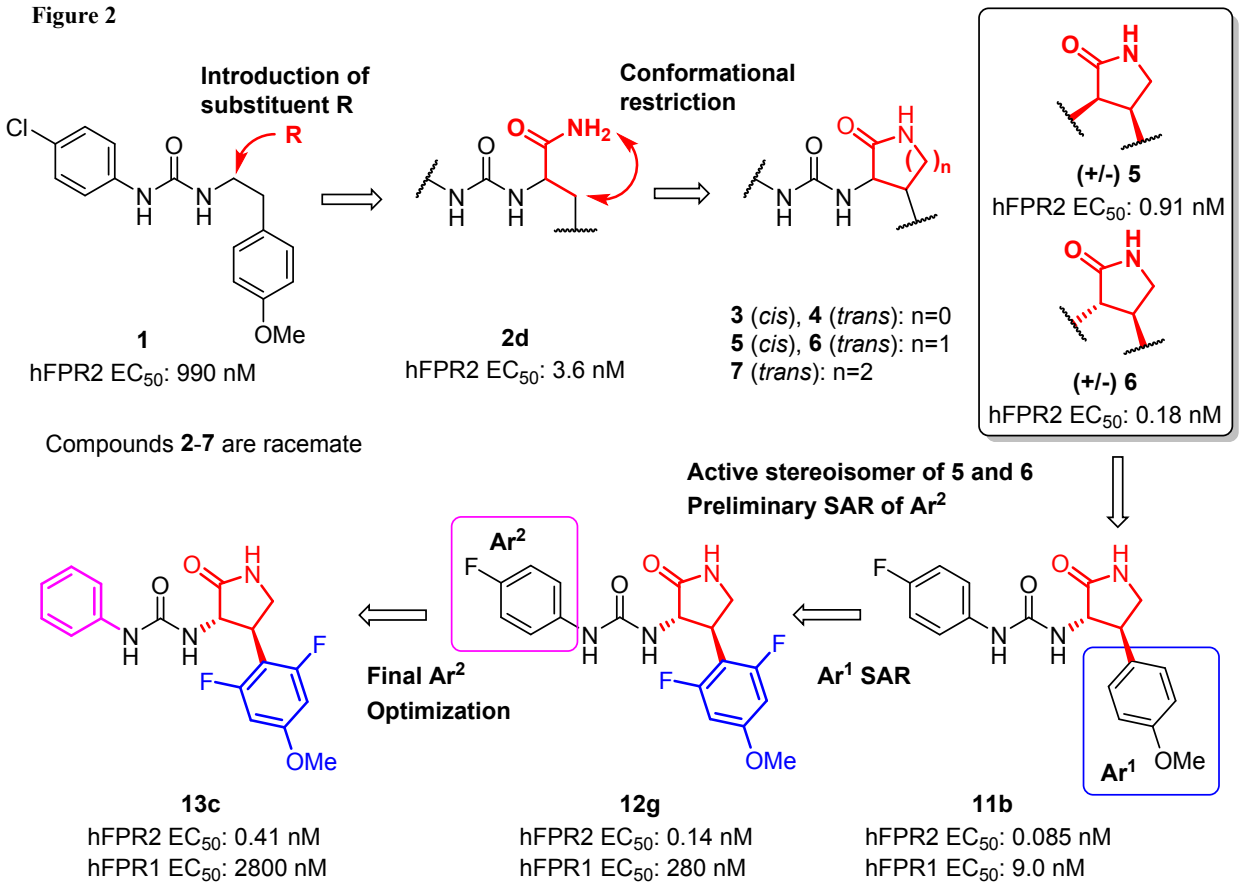

Results and Discussions

All synthesized compounds were evaluated for agonistic activity to induce Ca^{2+} mobilization in HEK293 cells over-expressing hFPR2 and HEK293 cells over-expressing hFPR1.

First, the hFPR2 agonistic activity of acyclic urea derivatives **1** and **2a–d** were evaluated to determine the effect of substitution on the 4-methoxyphenylethyl moiety (Table 1). Compound **1** showed weaker hFPR2 activity than that described in the literature, which may be due to assay conditions and expression levels of the receptor in the reporter cell lines. By contrast, compounds **2a–d** exhibited 32- to 275-fold more potent hFPR2 activity than **1**. Carbamoyl derivative **2d** exhibited the strongest hFPR2 activity (EC_{50} = 3.6 nM) and was selected as a template for structural modifications.

Table 1. Human FPR2 Agonist Activity for Acyclic Analogs

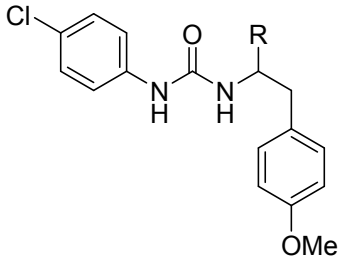

2 (racemate)

comp	R	hFPR2 $EC_{50}{}^{a}$ (nM)
1	H	990
2a	Me	23
2b	CH_2OH	6.8
2c	COOH	31
2d	$CONH_2$	3.6

[a]EC_{50} values were determined by Ca^{2+} mobilization in HEK293 cells over-expressing hFPR2.

We designed 4−6 membered lactam derivatives **3**−**7** to constrain the conformation of **2d** without changing the steric bulk of the carbamoyl moiety and the lipophilicity of the molecule. In addition to the hFPR2 activity of compounds **3**−**7**, the agonist activity for hFPR1 was measured to evaluate receptor selectivity (Table 2). The template compound **2d** had excellent hFPR2 selectivity (hFPR1/2 ratio >2800). The hFPR2 activity of *cis*- and *trans*-oriented azetidinone urea derivatives **3** and **4** were 3- to >28-fold less potent than **2d**. By contrast, *cis*- and *trans*-oriented pyrrolidinone urea derivatives and *trans*-oriented piperidinone derivative **5**−**7** were 4- to 33-fold more potent for hFPR2 over **2d**. However, hFPR1 activity of **5**−**7** also increased, and hFPR1/2 selectivity of these compounds was lower than that of **2d**.

Table 2. Activity of **3**−**7** in HEK293 Cells Expressing Human FPR2 and FPR1

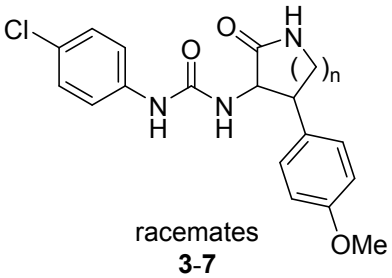

racemates
3-**7**

comp	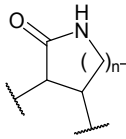	EC_{50} (nM)[a] hFPR2	hFPR1	ratio
2d		3.6	>10000	>2800
3	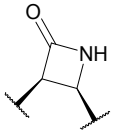	12	>10000	>830
4	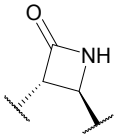	>100	>10000	NC[c]
5	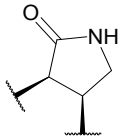	0.91	100	110
6	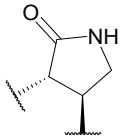	0.18	31	170
7	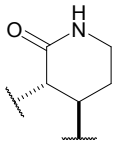	0.11	<10	<91

[a]EC_{50} values were determined by Ca^{2+} mobilization in HEK293 cells over-expressing hFPR2 or hFPR1. [c]Not calculated.

Based on the results described above, we selected pyrrolidinone derivatives **5** and **6** for further optimization since they offered the best combination of potency and selectivity. The four optically active isomers **8**−**10** and **11a** were assayed to ascertain the most active stereoisomer (Table 3). In the *cis*-oriented isomers, (+)-enantiomer **9** had 5-fold more potent hFPR2 activity than (-)- **8**. In the *trans*-oriented isomers, (3*S*,4*R*)-enantiomer **11a** was 360-fold more potent for hFPR2 than the (3*R*,4*S*)-enantiomer **10**. Comparing the hFPR2 activity of diastereomers **9** and **11a**, **11a** was 10-fold more active than **9**, demonstrating that the (3*S*,4*R*)-isomer was the most active stereoisomer. However, **11a** was only moderately selective over FPR1 (42x). Compound **11b** bearing a 4-fluorophenyl group had similar hFPR2 activity and selectivity to **11a**, so we selected **11b** as the lead compound for detailed structure activity relationship (SAR) studies to identify a candidate compound.

Table 3. Activity of **8**-**11** in HEK293 Cells Expressing Human FPR2 and FPR1

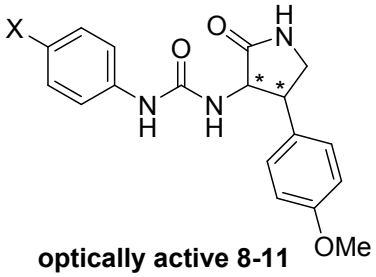

optically active 8-11

comp	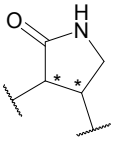	X	EC_{50} (nM)[a] hFPR2	EC_{50} (nM)[a] hFPR1	ratio
8	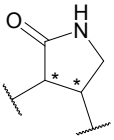 (-)-*cis*	Cl	4.6	950	210
9	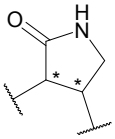 (+)-*cis*	Cl	0.90	81	90
10	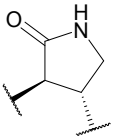	Cl	34	910	27
11a	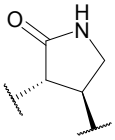	Cl	0.092	3.9	42
11b	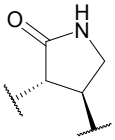	F	0.085	9.0	110

[a]EC_{50} values were determined by Ca^{2+} mobilization in HEK293 cells over-expressing hFPR2 or hFPR1.

After the core pyrrolidinone was selected, optimization of the 4-methoxyphenyl group was carried out (Table 4). Introduction of a fluorine atom to the 2- or 3-position of the 4-

methoxyphenyl group (**12a**, **12b**) resulted in 5- to 10-fold decreased hFPR2 activity relative to **11b** and did not improve hFPR2 selectivity. Furthermore, 2-chloro (**12c**), 2-methyl (**12d**) or 4-chloro (**12e**) analogs also had nanomolar hFPR2 activity. By contrast, compounds **12f** and **12g** with an additional fluorine atom at position 5 or 6 of **12a** maintained picomolar hFPR2 activity. Remarkably, a dramatic decrease in FPR1 activity was observed in the compound **12g** bearing 2,6-difluoro-4-methoxyphenyl group as Ar^1. Compound **12g** showed excellent hFPR2 activity (EC_{50} = 0.14 nM) and high hFPR2 selectivity (FPR1/2 ratio = 2000). Whereas the 3-fluoro-5-methoxypyridin-2-yl group (**12h**) maintained FPR2 activity, the selectivity over hFPR1 was reduced relative to **12g**. Furthermore, replacement of the 4-methoxy group of **12g** with an ethoxy (**12i**), an ethyl (**12j**), a cyano (**12k**) or a methylamino (**12l**) group resulted in a 10- to 700-fold decreased hFPR2 activity over **12g**.

Table 4. Activity of **12** in HEK293 Cells Expressing Human FPR2 and FPR1

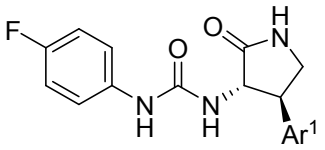

12

comp	Ar^1	EC_{50} (nM)[a] FPR2	EC_{50} (nM)[a] FPR1	ratio	comp	Ar^1	EC_{50} (nM)[a] FPR2	EC_{50} (nM)[a] FPR1	ratio
11b	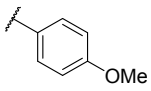	0.085	9.0	110	**12f**	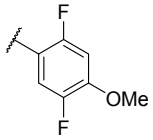	0.15	17	110
12a	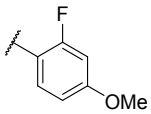	0.45	86	190	**12g**	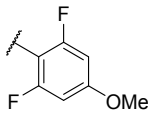	0.14	280	2000
12b	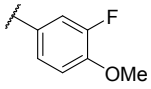	0.90	72	80	**12h**	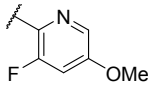	0.36	190	530
12c	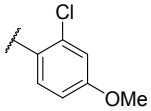	4.0	410	100	**12i**	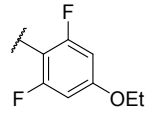	14	NT[b]	NC[c]
12d	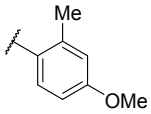	1.6	76	48	**12j**	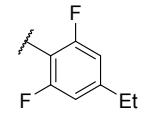	5.8	1500	260
12e	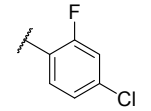	3.1	29	9.4	**12k**	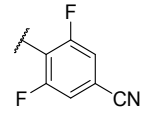	9.7	40000	4100
					12l	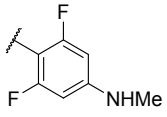	1.4	1900	1400

[a]EC_{50} values were determined by Ca^{2+} mobilization in HEK293 cells over-expressing hFPR2 or hFPR1. [b]Not tested. [c]Not calculated.

We next evaluated the substituent effect of Ar^2 for a series of 4-(2,6-difluoro-4-methoxyphenyl)pyrrolidinone derivatives **13a–q** (Table 5). The 3-fluorophenyl and 2-

fluorophenyl derivative **13a** and **13b** showed 7- and 310-fold less hFPR2 activity than **12g**. On the other hand, the phenyl, 4-chorophenyl, and 4-bromophenyl derivatives **13c−e** showed comparable hFPR2 activity to **12g**. Among these compounds, phenyl derivative **13c** showed higher hFPR2 selectivity (FPR1/2 = 6800) than **12g**. Other 4-position substituents, including cyano, methyl and methoxy derivatives **13f−h** were 6- to 23-fold less active than **12g**. The 3,4-disubstituted phenyl derivatives **13i−l** showed comparable hFPR2 activity to **12g**. Among these compounds 3,4-difluorophenyl derivative **13i** and 3-hydroxy-4-methylphenyl derivative **13l** showed higher hFPR2 selectivity (hFPR1/2 = 5100 and 13000, respectively) than **12g**. Although, the aromatic heterocycle derivatives **13m−q** showed 2- to 32-fold reduced activity compared to **12g**, 5-chlorothiophen-2-yl derivative **13n** showed good hFPR2 activity (EC_{50} = 0.29 nM), and higher hFPR2 selectivity (FPR1/2 = 4100) than **12g**.

Table 5. Activity of **13a-q** in HEK293 Cells Expressing Human FPR2 and FPR1

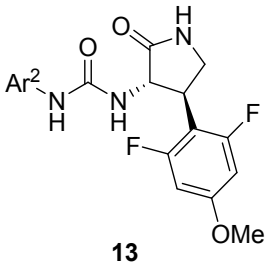

13

comp	Ar^2	EC$_{50}$ (nM)[a] FPR2	EC$_{50}$ (nM)[a] FPR1	ratio	comp	Ar^2	EC$_{50}$ (nM)[a] FPR2	EC$_{50}$ (nM)[a] FPR1	ratio
12g	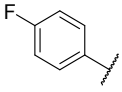	0.14	280	2000	**13i**	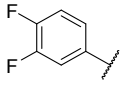	0.16	820	5100
13a	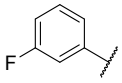	0.95	1700	1800	**13j**	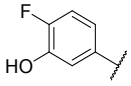	0.087	72	830
13b	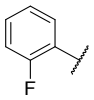	43	NT[b]	NC[c]	**13k**	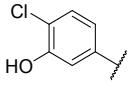	0.050	40	800
13c		0.41	2800	6800	**13l**	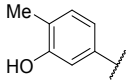	0.078	1000	13000
13d	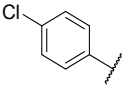	0.11	120	1100	**13m**	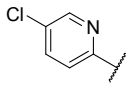	4.5	6900	1500
13e	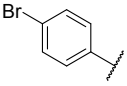	0.19	96	510	**13n**	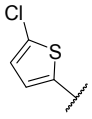	0.29	1200	4100
13f	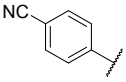	0.78	350	450	**13o**	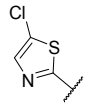	1.9	NT[b]	NC[c]
13g	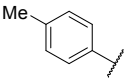	2.0	3200	1600	**13p**	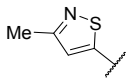	0.32	290	910
13h	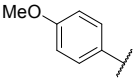	3.2	1000	310	**13q**	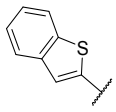	0.76	3000	3900

[a]EC$_{50}$ values were determined by Ca^{2+} mobilization in HEK293 cells over-expressing hFPR2 or hFPR1. [b]Not tested. [c]Not calculated.

Finally, to select a candidate compound, in vivo efficacy and CYP3A4 inhibition were evaluated for 5 analogs, **12g**, **13c**, **13i**, **13l**, and **13n**, which had potent in vitro hFPR2 activity (EC_{50} < 0.50 nM) and high hFPR2 selectivity (hFPR1/2 > 2000). In vivo efficacy was evaluated in a mouse inflammation model by measuring inhibition of neutrophil infiltration into lung after oral administration at 1 mg/kg (Table 6). The 4-fluorophenyl derivative **12g**, phenyl derivative **13c** and 5-chlorothiophen-2-yl derivative **13n** showed excellent in vivo efficacy (inhibition >80%), while the disubstituted phenyl derivatives **13i** and **13l** showed weaker in vivo efficacy.

Among the three compounds that inhibited neutrophil infiltration in mice, selection for advanced in vivo studies relied on several factors. Analog **13n** was excluded as a candidate compound due CYP3A4 inhibition. Higher FPR2 selectivity in the Ca^{2+} flux assay was measured for **13c** versus **12g** (6800 vs 2000 fold, Table 5); in addition, only oxidative metabolites were observed after hepatocyte incubation with **13c**, while oxidative defluorination was observed with **12g** (data not provided). Based on these differences, **13c** was progressed to additional studies.

Table 6. Effect of Selected Compounds on LPS-induced Neutrophil Infiltration in Mouse Lungs

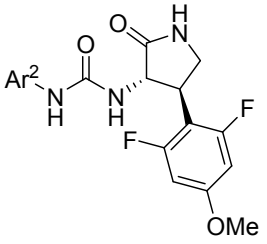

12g, 13c,i,l,n

compd	Ar^2	FPR2 EC_{50} (nM)[a]		In vivo inhibition (%)[b]	CYP inhibition IC_{50} (μM)[c]
		human	mouse		
12g	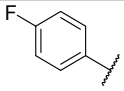	0.14	1.5	97	>20
13c		0.41	3.4	88	>20
13i	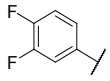	0.16	8.5	4.9	>20
13l	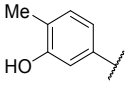	0.078	0.63	55	>20
13n	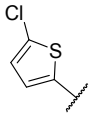	0.29	1.4	84	5.6

[a]EC_{50} values were determined by Ca^{2+} mobilization in HEK293 cells over-expressing hFPR2 or mFPR2. [b]Inhibition (%) was determined by measurement of neutrophils in BALF of LPS-dosed mice after oral dosing of 1 mg / kg. [c]IC_{50} values were determined with recombinant human CYP3A4.

Additional in vitro assays examined more detailed cellular signaling of FPR2 agonist **13c** (Table 7). Inhibition of cAMP levels was observed in cells over-expressing either hFPR2 or hFPR1, consistent with G_i coupling, with an 80x selectivity for hFPR2. β-Arrestin recruitment was also observed. Potency was right shifted in both assays compared to calcium mobilization, which could be due to different assay conditions, including the level of receptor expression in the cell lines. Confirming cross species selectivity, **13c** demonstrated 1000x selectivity for FPR2 over FPR1 in the cAMP assay using CHO cells over-expressing the mouse receptors. The impact on inflammatory cells was measured in two key cellular assays: Compound **13c** inhibited chemotaxis of a neutrophil-like cell line against a gradient of SAA and stimulated phagocytosis by mouse macrophages at low nanomolar potency. These assays show the potential of FPR2 agonists to prevent pro-inflammatory neutrophil infiltration, and the ability to promote a wound healing phenotype in macrophages, which are key characteristics of compounds that stimulate resolution of inflammation.

Table 7. Mechanistic in vitro assays **13c**

Assay	EC_{50} or $IC_{50}{}^{a}$ (nM)
hFPR2 cAMP	5.0
hFPR1 cAMP	400
mFPR2 cAMP	0.5
mFPR1 cAMP	500
β-Arrestin Recruitment	130
Chemotaxis	57

Phagocytosis	<1

[a]EC_{50} values for cAMP were determined in Chinese Hamster Ovary cells (CHO) over-expressing hFPR1, hFPR2, mFPR1 or mFPR2 receptors. β-Arrestin values were measured in a DiscoverX Pathhunter® cell line. Phagocytosis assays used mouse peritoneal macrophages. IC_{50} value for the chemotaxis assays used a HL-60 cell line.

In vivo pharmacokinetic (PK) data and in vitro intrinsic clearance values in liver microsomes and hepatocytes for compound **13c** are listed in Table 8. Compound **13c** had high clearance in rat and mouse, but moderate clearance in dog and monkey with good bioavailability. The clearance values in human microsomes and human hepatocytes were about 10-fold lower than those of rat, dog and monkey, suggesting that **13c** is more metabolically stable in humans than in these animal species.

Table 8. Cross Species Comparison of In Vivo PK Parameters and In Vitro Intrinsic CL of **13c**

Species	i.v.			p.o.					Liver microsome int.CL[f]	Hepatocyte int.CL[g]
	Dose[a]	V_{dss}[b]	CL_{tot}[c]	Dose[a]	C_{max}[d]	$T_{1/2}$ (h)	AUC_{0-inf}[e]	BA (%)		
Mouse	0.5	3.5	90	1.0	160	0.68	120	24	NT[h]	NT[h]
Rat	1.0	3.0	49	1.0	240	3.8	640	67	0.021	15
Dog	1.0	0.98	6.6	1.0	820	2.5	5700	50	0.042	50
Monkey	1.0	1.2	12	3.0	800	5.0	5800	49	0.030	28
Human	NT[h]	NT[h]	NT[h]	NT[h]	NT[h]	NT[h]	NT[h]	NT[h]	0.0033	3.5

[a]Dose is expressed in mg/kg. [b]V_{dss} is expressed in L/kg. [c]CL_{tot} is expressed in mL/min/kg. [d]C_{max} is expressed in nmol/L. [e]AUC_{0-inf} is expressed in nmol/L · h. [f]CL is expressed in mL/min/mg protein. [g]CL is expressed in mL/min/kg. [h]Not tested

A major cause of heart failure is adverse cardiac remodeling post myocardial infarction (MI) during a period characterized by dysregulated chronic inflammation. FPR2 agonists have the potential to resolve this inflammation and improve cardiac structure and function. To investigate the role of FPR2 agonism in the setting of heart failure, the selective FPR2 agonist **13c** was evaluated in a mouse model of myocardial infarction (MI), which leads to heart failure develpment. In these studies, the left anterior descending (LAD) artery was permanently occluded with a surgical suture. Non-infarcted surgical sham mice had sutures placed around the LAD artery but not tightened. The lowest dose of **13c** that showed a significant effect on IL-10 stimulation (0.3 mg/kg) in mice treated with LPS was selected for testing in the myocardial infarction model. Vehicle and **13c** were dosed daily

by oral gavage for 24 days starting 4 days post MI. The angiotensin converting enzyme inhibitor (ACEi), captopril, was provided in the drinking water (~ 100 mg/kg/day) to compare a standard of care therapy for acute MI.

After 28 days, infarct scar expansion and left ventricular chamber remodeling were evaluated. The passive mechanics of the left ventricle (LV) were analyzed using a modified Langendorff apparatus. A deflated balloon attached to a pressure transducer was inserted into the LV cavity. The passive compliance of the left ventricle was evaluated following three inflation and deflation cycles of the balloon. Figure 4A shows mean left ventricular pressure–volume (P–V) curves obtained from the various treatment groups as well as surgical sham mice. Treatment with vehicle yielded a right-shifted P-V curve relative to non-infarcted sham hearts shown at the left of the plot. The results indicate that infarcted mouse hearts treated with vehicle have dilated LV chambers at each measured pressure. By contrast, the P-V curve obtained with the FPR2 agonist **13c** is left shifted relative to vehicle, indicating smaller LV chambers with treatment. Treatment with captopril also yielded a left shifted P-V curve relative to vehicle, but to a lesser degree than that obtained with compound **13c**. The findings suggest that LV chamber remodeling

is attenuated with both compound **13c** and captopril treatments post MI. Heart weights for compound **13c** and captopril treatment groups were reduced relative to the vehicle group (Figure 4B). These findings indicate that compound **13c** can attenuate left ventricle and global cardiac remodeling.

Figure 4: Effect of **13c** and captopril (ACEi) treatment on myocardial structure and function post LAD in mice. A) Left ventricular pressure-volume curves. B) Heart weights 28 days post MI. C) Representative heart cross-sections by histology depicting the degree of myocardial infarction. Non-infarcted surgical sham animals are shown for comparisons. D) Scar length 28 days post MI. Doses: 13c, 0.3 mg/kg/d; captoril, 100 mg/kg/d.

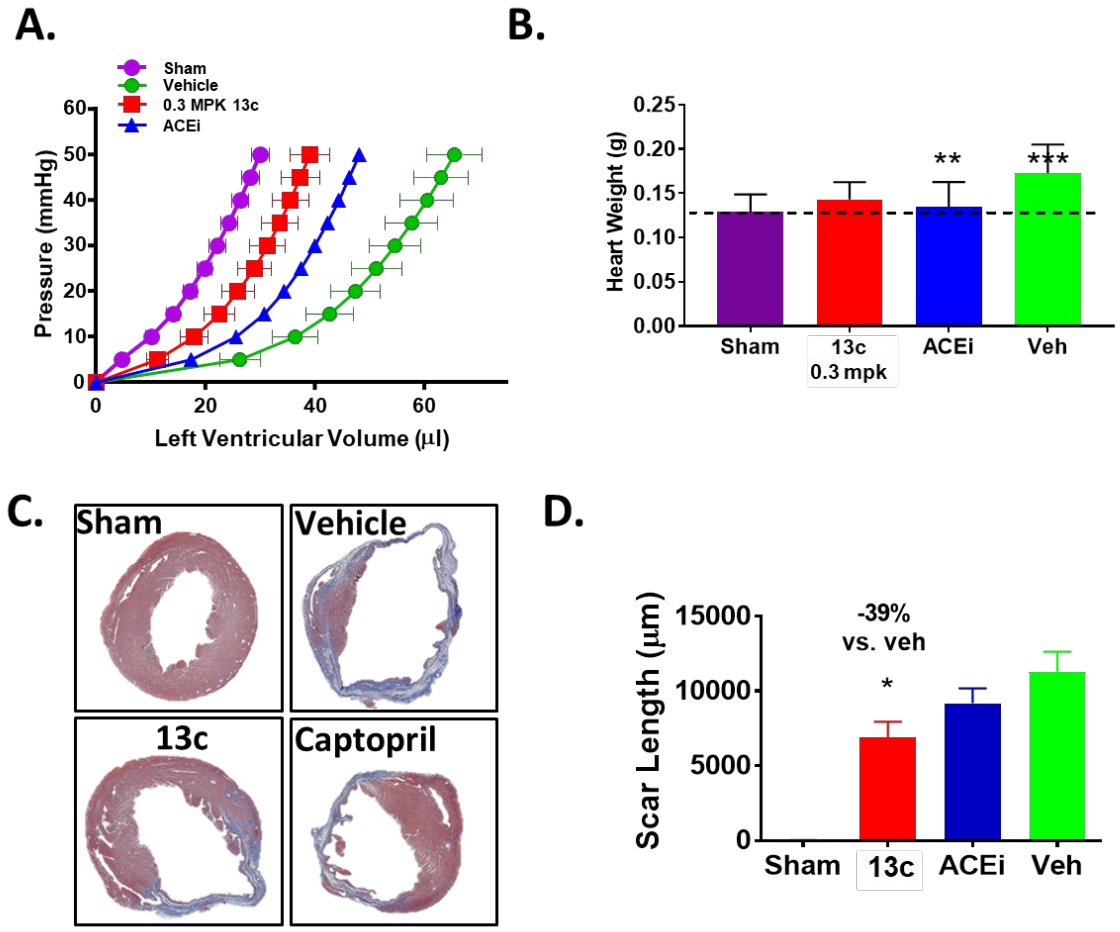

Cross sections of the left ventricle were analyzed for histomorphometric assessments of infarct structure. Representative images showing the size of the MI and LV chambers are shown for all groups (Figure 4C). Infarct length was quantified for all groups as an indicator of overall scar expansion. As shown in Figure 4D, vehicle-treated mice yielded the largest scar lengths. By contrast, treatment with compound **13c** reduced infarct length by 39% relative to vehicle ($P<0.05$). Despite the decreases in heart weight and decreased

LV chamber areas noted in Figure 4A and B, treatment with captopril was unable to reduce scar length to a degree similar to that obtained with compound **13c**.

Chemistry

The synthesis of racemic *cis*- and *trans*-oriented azetidine urea derivatives **3** and **4** are shown in Scheme 1. Reaction of imine **14** with 2-(1,3-dioxoisoindolin-2-yl)acetyl chloride in the presence of triethylamine, gave **15**[23] as the mixture of *cis* and *trans* isomers. Removal of the 4-methoxyphenyl group of **15** with cerium (IV) ammonium nitrate (CAN) provided *cis* isomer **16**. Treatment of **16** with hydrazine monohydrate, followed by treatment with HCl, gave **17**. Reaction of **17** with 4-chlorophenyl isocyanate in the presence of saturated aqueous sodium hydrogen carbonate provided *cis*-oriented **3**. Azidation of a hydroxyl group of *cis*-isomer **18**,[24] followed by deprotection of the 4-methoxyphenyl group of t*rans*-**19** with CAN, gave **20**. A Staudinger reaction followed by treatment with 4-chlorophenyl isocyanate, provided *trans*-oriented **4**. The stereochemistry of the C-3 and C-4 positions of all compounds was determined by comparison of coupling

constant of the C-3 and C-4 hydrogen atom in the ^{1}H NMR ($J_{3,4}$>4.0 Hz for the *cis* isomer, $J_{3,4}$<3.0 Hz for the *trans* isomer).[25]

Scheme 1. Synthesis of Azetidinone Urea Derivatives **3** and **4**[a]

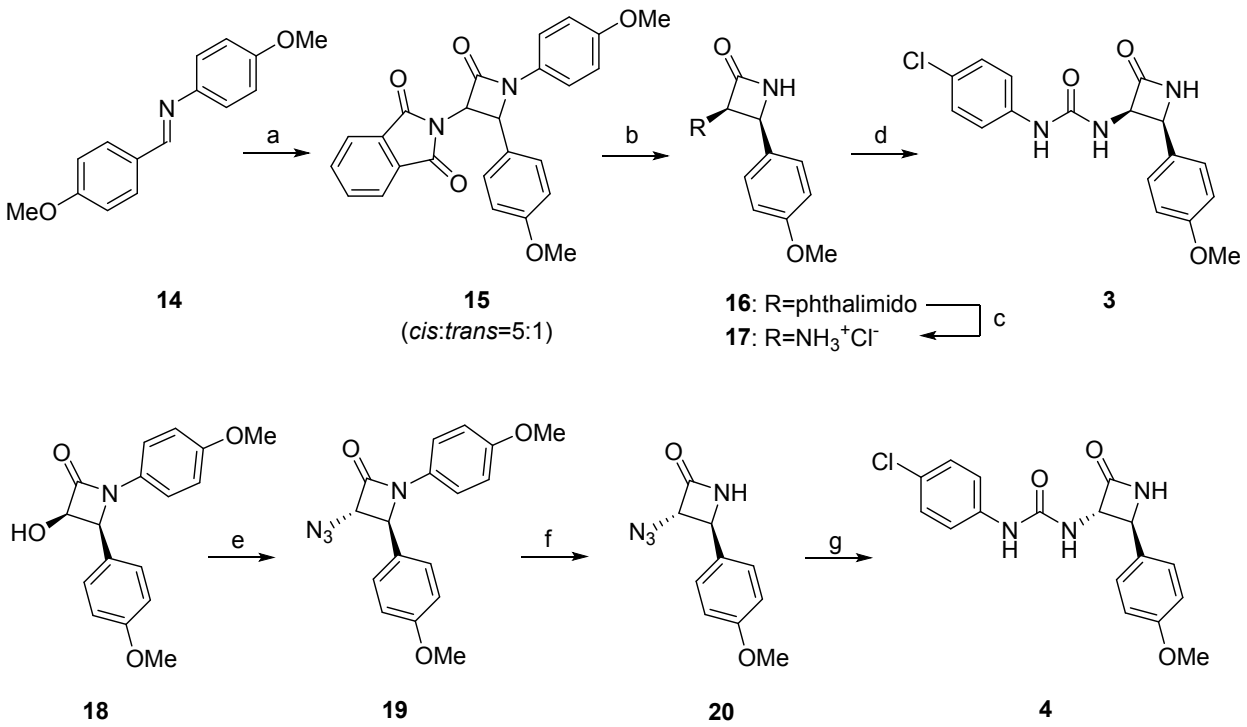

Compounds **3**, **4**, **15**-**20** are racemic.

[a]Reagents and conditions: (a) 2-(1,3-dioxoisoindolin-2-yl)acetyl chloride, Et_3N, CH_2Cl_2, 28%; (b) CAN, MeCN-THF-H_2O, 62%; (c) (1) hydrazine monohydrate, dioxane, (2) HCl, 53%; (d) 4-chlorophenyl isocyanate, sat $NaHCO_3$ aq., AcOEt, 63%; (e) (1) MsCl, Et_3N, (2) NaN_3, DMF, 89%; (f) CAN, MeCN, 85%; (g) (1) PPh_3, THF (2) H_2O (3) 4-chlorophenyl isocyanate, 48% (three steps) .

The synthesis of racemic *cis*- and *trans*-oriented pyrrolidinone urea derivatives **5** and **6** (Scheme 2) began with the reaction of **21**[26] and *tert*-butyl (2,2,2-trifluoroacetyl)glycinate

in the presence of lithium *bis*(trimethylsilyl)amide (LHMDS) to give compound **22**. After removal of the *tert*-butyl ester group with trifluoroacetic acid (TFA), treatment of **23** with iodomethane in the presence of potassium hydrogen carbonate provided **24**. Reduction of the nitro group using zinc powder and ammonium chloride, followed by treatment with titanium(III) chloride and sodium acetate,[27] gave pyrrolidinone **25** as a *cis* and *trans* mixture. Removal of the trifluoroacetyl group under basic conditions and subsequent treatment of **26** with 4-chlorophenyl isocyanate, was followed by separation of the diastereomers by column chromatography, to provide *cis*-oriented **5** and *trans*-oriented **6**.

Scheme 2. Synthesis of Pyrrolidinone Urea Derivatives **5** and **6**[a]

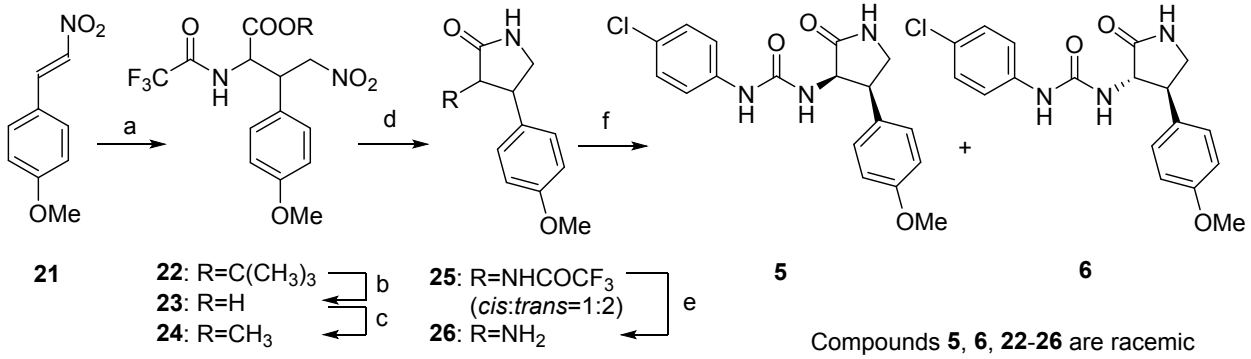

[a]Reagents and conditions: (a) *tert*-butyl (2,2,2-trifluoroacetyl)glycinate, LHMDS, THF, 88%; (b) TFA, 58%.; (c) MeI, $KHCO_3$, DMF, 92%; (d) (1) Zn, NH_4Cl, MeOH-H_2O, (2) 20%

$TiCl_3$, NaOAc, MeOH-H_2O 63% (two steps); (e) 1 M aq. NaOH, MeOH; (f) 4-chlorophenyl isocyanate, EtOAc, 4% (two steps for **5**), 44% (2 steps for **6**).

Racemic *trans*-oriented piperidinone urea derivative **7** (Scheme 3) was synthesized by conjugate addition of dimethyl malonate to compound **27** in the presence of sodium methoxide,[28] followed by reduction of the cyano group in **28** using nickel boride to give piperidinone **29**. After hydrolysis of ester **29** under basic conditions, treatment of **30** with diphenylphosphoryl azide (DPPA) in the presence of triethylamine, followed by the reaction with 4-chloroaniline provided piperidinone **7**.

Scheme 3. Synthesis of Piperidinone Urea Derivative **7**[a]

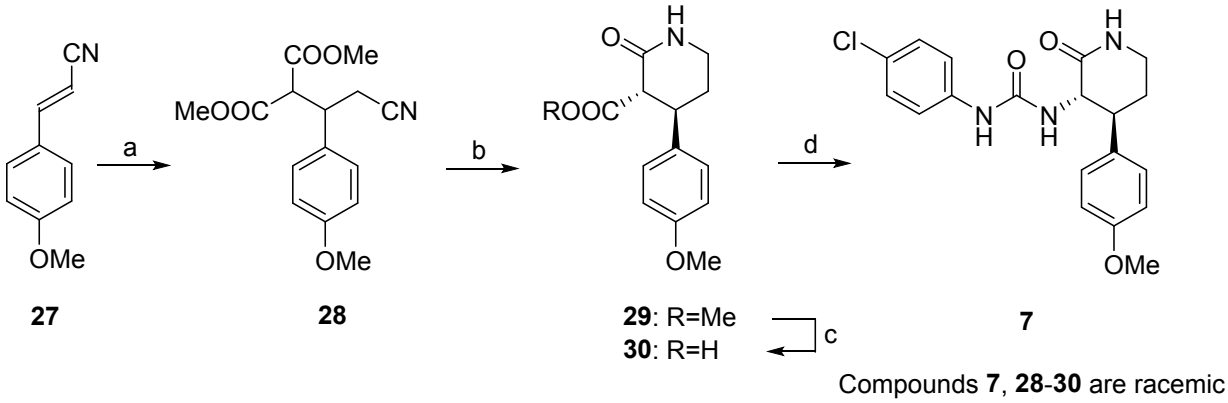

[a]Reagents and conditions: (a) Dimethyl malonate, NaOMe, MeOH, 24%; (b) $NaBH_4$, $NiCl_2 \cdot 6H_2O$, MeOH, 65%; (c) 1 M NaOH, MeOH, 92%; (d) DPPA, Et_3N, toluene then 4-chloroaniline (6.5%).

The synthesis of optically active *cis*-oriented pyrrolidinone urea derivatives **8** and **9** is shown in Scheme 4. After the reaction of **21** with ethyl 2-[(diphenylmethylene)amino]acetate in the presence of lithium diisopropylamide (LDA), removal of the diphenylmethylene group under acidic condition, followed by treatment with di-*tert*-butyl dicarbonate (Boc_2O) in the presence of saturated aqueous sodium hydrogen carbonate gave **31**. Reduction of the nitro group with nickel boride, followed by isolation of enantiomers using HPLC chromatography (CHIRALPAK ID), gave (-)-*cis*-isomer **32** and (+)-*cis*-isomer **33**. Deprotection of the Boc group of **32** and **33** under acidic conditions, followed by treatment with 4-chlorophenyl isocyanate in the presence of saturated aqueous sodium hydrogen carbonate, gave (-)-*cis*-isomer **8** and (+)-*cis*-isomer **9**, respectively.

Scheme 4. Synthesis of Optically Active *Cis*-oriented Pyrrolidinone Urea Derivatives **8** and **9**[a]

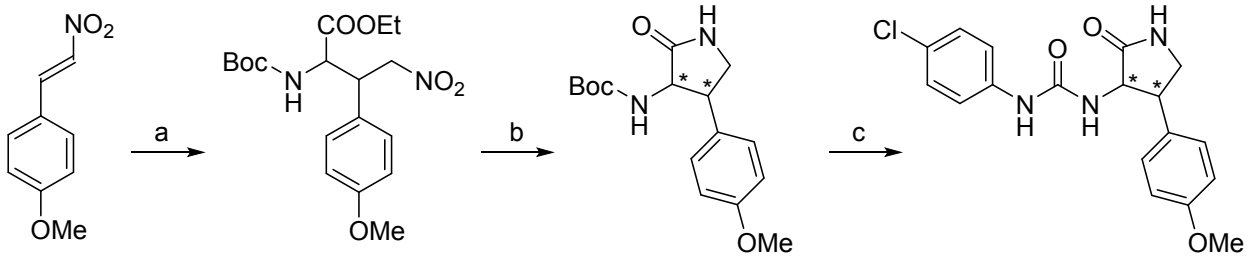

21 **31 (racemate)** **32 [(-)-*cis*]** **33 [(+)-*cis*]** **8 [(-)-*cis*]** **9 [(+)-*cis*]**

[a]Reagents and conditions: (a) (1) ethyl 2-[(diphenylmethylene)amino]acetate, LDA, THF , (2) AcOH, H_2O, (3) Boc_2O, $NaHCO_3$ aq., THF, 63% (three steps); (b) (1) $NaBH_4$, $NiCl_2 \cdot 6H_2O$, MeOH, 84% (2) HPLC separation, CHIRALPAK ID, 35% (for **32**), 43% (for **33**); (c) (1)TFA, CH_2Cl_2, (2) 4-chlorophenyl isocyanate, sat $NaHCO_3$, THF, 56% (two steps for **8**), 56% (two steps for **9**).

The synthesis of *trans*-oriented (3*R*,4*S*)- and (3*S*,4*R*)-pyrrolidinone urea derivatives **10** and **11** is shown in Scheme 5. Enantioselective Michael addition[29] of dimethyl malonate to **21** using Ni(II)-*bis*[(*R*,*R*)-*N*,*N*-dibenzylcyclohexane-1,2-diamine]bromide[29a] followed by reduction of the nitro group using nickel boride, gave (3*R*,4*S*)-isomer **35**. After hydrolysis of ester **35** under basic condition, reaction of acid **36** with DPPA in the presence of triethylamine, followed by treatment with 4-chloroaniline, provided (3*R*, 4*S*)-isomer **10**. The (3*S*,4*R*)-isomer **38** was synthesized in the same manner as described for **35** using Ni(II)-*bis*[(*S*,*S*)-*N*,*N*-dibenzylcyclohexane-1,2-diamine]bromide as the catalyst. After hydrolysis of ester **38** under basic condition, reaction with DPPA in the presence of

triethylamine, followed by the treatment with 4-chloroaniline or 4-fluoroaniline, gave **11a** and **11b** respectively.

Scheme 5. Synthesis of Optically Active *Trans*-oriented Pyrrolidinone Ureas **10** and **11**[a]

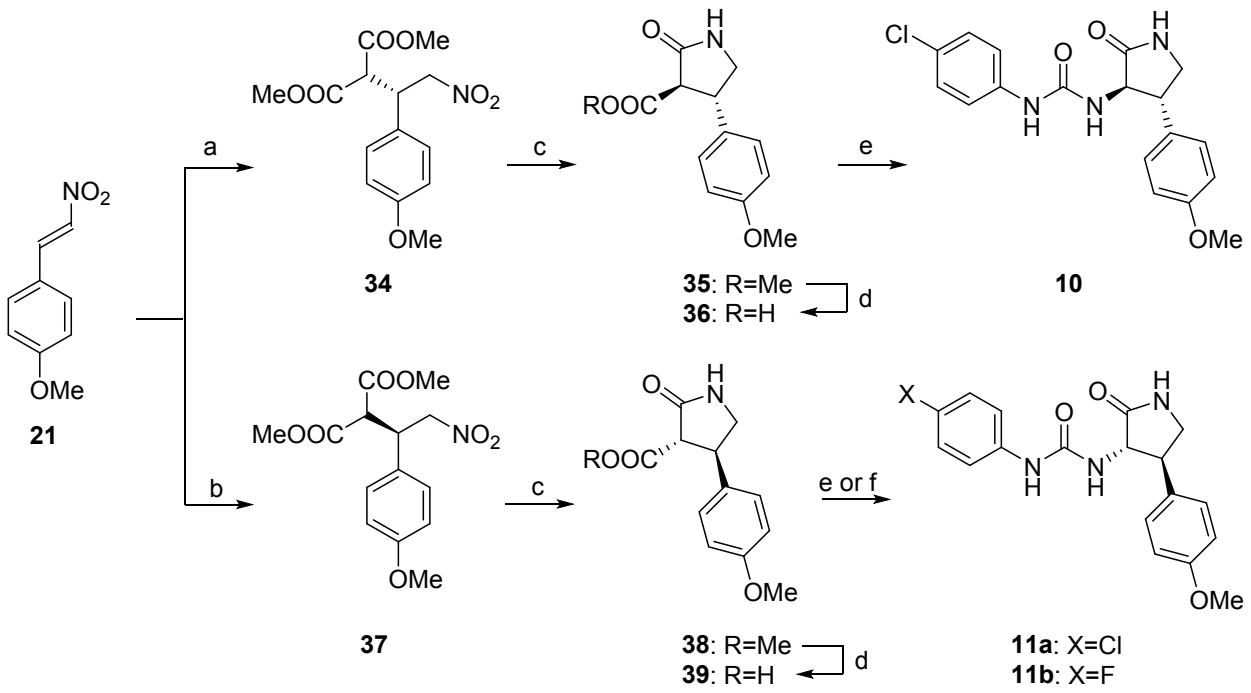

[a]Reagents and conditions: (a) Dimethyl malonate, Ni(II)-*bis*[(*R*,*R*)-*N*,*N*-dibenzylcyclohexane-1,2-diamine]bromide (3 mol%), toluene; (b) Dimethyl malonate, Ni(II)-*bis*[(*S*,*S*)-*N*,*N*-dibenzylcyclohexane-1,2-diamine]bromide (3 mol%), toluene; (c) $NaBH_4$, $NiCl_2 \cdot 6H_2O$, MeOH, 73% (two steps for **35**), 68% (two steps for **38**); (d) 1 M NaOH aq., MeOH, 88%, (for **36**), 98% (for **39**); (e) DPPA, Et_3N, toluene then 4-chloroaniline, 53% (for **10**), 24% (for **11a**); (f) DPPA, Et_3N, toluene then 4-fluoroaniline, 18% (for **11b**).

The synthesis of the selected compounds **12g**, **13c**, **13i**, **13l** and **13n** is shown in Scheme 6. Treatment of **40** with $MeNO_2$ in the presence of ammonium acetate[30], gave nitrostyrene **41**, that was converted to carboxy derivative **44** in the same manner as described for **39**. Conversion of **44** to *N*-Cbz derivative **45** by a Curtius rearrangement, and removal of the Cbz group by catalytic hydrogenation, gave amino derivative **46**. Reaction of **44** with DPPA in the presence of triethylamine, followed by treatment with 4-fluoroaniline or 5-amino-2-methylphenol, gave **12g** and **13l** respectively. Reaction of **46** with phenyl isocyanate or 2,4-difluorophenyl isocyanate, gave **13c** and **13i** respectively. Treatment of **46** with 2-chlorothiophene-5-carboxylic acid in the presence of DPPA and triethylamine, gave **13n**.

Scheme 6. Synthesis of Selected Compounds **12g**, **13c**, **13i**, **13l** and **13n**[a]

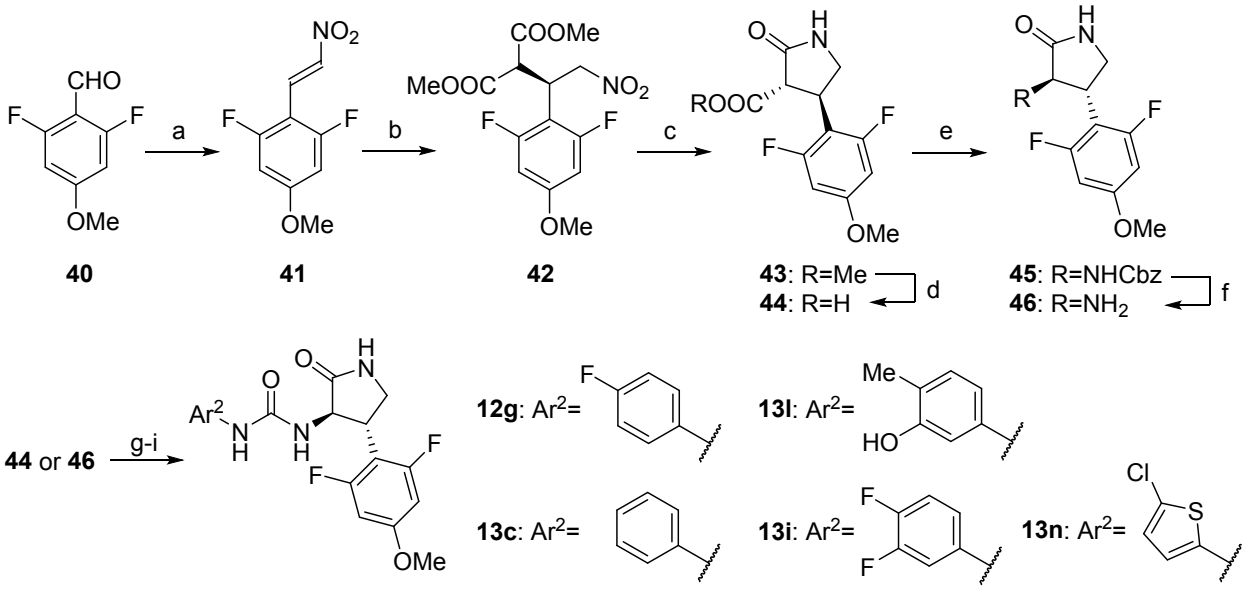

[a]Reagents and conditions: (a) $MeNO_2$, ammonium acetate, AcOH, 95%; (b) dimethyl malonate, Ni(II)-*bis*[(*S*,*S*)-*N*,*N*'-dibenzylcyclohexane-1,2-diamine]bromide (3 mol%), toluene, 95%; (c) $NaBH_4$, $NiCl_2 \cdot 6H_2O$, MeOH, 55%; (d) 1 M NaOH aq., MeOH, 99%; (e) DPPA, Et_3N, toluene then BnOH, 47%; (f) H_2, 10% Pd-C, EtOH, 100%; (g) **44**, DPPA, Et_3N, toluene then 4-fluoroaniline or 5-amino-2-methylphenol, 55% (for **12g**), 65% (for **13l**); (h) **46**, phenyl isocyanate or 3,4-difluorophenyl isocyanate, THF, 76% (for **13c**), 86% (for **13i**); (i) **46**, 2-chlorothiophene-5-carboxylic acid, DPPA, Et_3N, toluene, 38% (for **13n**).

Other analogs were synthesized using analogous chemistry and details are provided in the supporting information section.

Conclusion

Conformational restriction of a simple phenylethyl urea FPR2 agonist led to the discovery of a pyrrolidinone core, which was further optimized to produce potent FPR2 agonists with selectivity over FPR1. Evaluation of lead compounds in a lung LPS model and metabolic profilng assays led to the identification of compound **13c** (BMS-986235/LAR-1219) as a clinical candidate. Compound **13c** showed robust efficacy on both structure and function endpoints in a mouse myocardial infarction heart failure model after oral dosing for 28 days. These findings suggest that this selective, orally bioavailable small molecule FPR2 agonist could prevent adverse pathological remodeling that leads to heart failure.

Experimental Section

Chemistry

Melting points were measured on an OptiMelt automated meltiong point system MPA100 without correction. Infrared spectra (IR) were recorded with a ParkinElmer Spectrum 100 spectrometer. Measurements of mass spectra (MS) and high resolution MS (HRMS) were performed with a JEOL JMS SX-102A or a JEOL JMS-T100LP mass spectrometer. Proton nuclear magnetic resonance (^{1}H NMR) spectra were measured with a JEOL JMN-EX400 (400 MHz) or a JEOL JMN-ECA-400 (400 MHz) spectrometer. The chemical shifts are expressed in parts per million (δ value) downfield from tetramethylsilane, using tetramethylsilane (δ = 0) and/or residual solvents such as chloroform (δ = 7.26) as an internal standard. Splitting patterns are indicated as follows: s, singlet; d, doublet; t, triplet; q, quartet; m, multiplet; br; broad peak. Specific optical rotations were measured on a JASCO P-1000 polarimeter. Purity data were collected by an Agilent 1100 HPLC with Agilent G1315B diode array detector. The column was used was a RP-AQUA (50 mm × 2.1 mm i.d., 2.6 μm, ChromaNik Technologies Inc., Japan) with a temperature of 45 °C and a flow rate of 0.5 mL/min. Mobile phase A and B were a mixture of 0.05% formic acid in water, and 0.05% formic acid in MeCN, respectively. The ratio of mobile phase was increased lineally from 5% to 95% over 5 min, 95% over the

next 3 min. The data for elemental analysis were within ±0.4% of the theoretical values and were determined by a Yanaco micro corder JM11. Column chromatography was carried out with silica gel [silica gel 60 (Kanto)] as an absorbent. Merck precoated thin layer chromatography (TLC) plates (silica gel 60 F_{254}, 0.25 mm, Art 5715) were used for the TLC analysis. All purities for final compounds are ≥95.0% and were measured using HPLC.

2-[1,2-*Bis*(4-methoxyphenyl)-4-oxoazetidin-3-yl]isoindoline-1,3-dione (15). A solution of 2-(1,3-dioxoisoindolin-2-yl)acetyl chloride (2.00 g, 8.94 mmol) in CH_2Cl_2 was added dropwise to a mixture of **14** (1.44 g, 5.87 mmol), triethylamine (2.7 mL, 19 mmol), and CH_2Cl_2 (65 mL) under cooling with NaCl−ice, and the mixture was stirred at room temperature for 38 h, and concentrated in vacuo. Flash chromatography (hexane/AcOEt = 2:1) of the residue gave **15** (718 mg, 28%). ^{1}H NMR ($CDCl_3$) *δ*: 3.66 (s, 2.5H, OCH_3 of major isomer), 3.74 (s, 0.5H, OCH_3 of minor isomer), 3.75 (s, 0.5H, OCH_3 of minor isomer), 3.79 (s, 2.5H, OCH_3 of major isomer), 5.26 (d, *J* = 2.4 Hz, 0.2H, C−4H of minor isomer), 5.30 (d, *J* = 3.0 Hz, 0.2H, C−3H of minor isomer), 5.40 (d, *J* = 5.4 Hz, 0.8H, C−4H of major isomer), 5.62 (d, *J* = 5.4 Hz, 0.8H, C−3H of major isomer), 6.65 (d, *J* = 8.5 Hz,

0.3H, ArH of minor isomer), 6.70−6.76 (m, 1.7H, ArH of major isomer), 6.81 (d, J = 9.1 Hz, 0.3H, ArH of minor isomer), 6.86 (d, J = 9.1 Hz, 1.7H, ArH of major isomer), 6.91 (d, J = 8.5 Hz, 0.3H, ArH of minor isomer), 7.18 (d, J = 8.5 Hz, 1.7H, ArH of major isomer), 7.27−7.31 (m, 0.3H, ArH of minor isomer), 7.39 (d, J = 9.1 Hz, 1.7H, ArH of major isomer), 7.63−7.67 (m, 1.7H, ArH of major isomer), 7.69−7.72 (m, 1.7H, ArH of major isomer), 7.76 (dd, J = 5.5, 3.0 Hz, 0.3H, ArH of minor isomer), 7.88 (dd, J = 5.5, 3.0 Hz, 0.3H, ArH of minor isomer).

2-[*cis*-2-(4-Methoxyphenyl)-4-oxoazetidin-3-yl]isoindoline-1,3-dione (16). A solution of ammonium cerium(IV) nitrate (2.33 g, 4.25 mmol) in water (14 mL) was added to a mixture of **15** (608 mg, 1.42 mmol), MeCN (28 mL) and THF (7 mL) under cooling with NaCl−ice, and the mixture was stirred at same temperature for 2 h, and then at room temperature for 2 h. After quenching the reaction addition of water, the mixture was extracted with AcOEt (3 × 40 mL). The combined extracts were washed with saturated aqueous $NaHCO_3$ solution, 10% aqueous $NaHSO_3$ solution, and brine, dried over anhydrous Na_2SO_4, filtered, and concentrated in vacuo. Flash chromatography (hexane/AcOEt = 2:1 → 1:2) of the residue gave **16** (283 mg, 62%) as a pale yellow amorphous solid. ^{1}H

NMR ($CDCl_3$) δ: 3.68 (s, 3H), 5.13 (d, J = 5.4 Hz, 1H), 5.56 (dd, J = 4.8, 1.8 Hz, 1H), 6.44 (br s, 1H), 6.75 (d, J = 8.5 Hz, 2H), 7.21 (d, J = 8.5 Hz, 2H), 7.63−7.66 (m, 2H), 7.68−7.72 (m, 2H). MS (FI^+) *m/z*: 322 (M^+). HRMS (FI^+) for $C_{18}H_{14}N_2O_4$ (M^+): calcd, 322.09536; found, 322.09543. IR (ATR) cm^{-1}: 3280, 1760, 1717.

***cis*-3-Amino-4-(4-methoxyphenyl)azetidin-2-one Hydrochloride (17).** A solution of hydrazine monohydrate (0.050 mL, 1.0 mmol) in MeOH (0.3 mL) was added to a solution of **16** (250 mg, 0.776 mmol) in 1,4-dioxane (3.1 mL), the mixture was stirred at room temperature for 1 h, and concentrated in vacuo. After addition of MeOH (3.0 mL) and 1 M HCl (1.5 mL) to the residue, the mixture was stirred at 40 °C for 2 h, and concentrated in vacuo. After addition of water to the residue, the insoluble materials were filtered off, and then the filtrate was concentrated in vacuo. After addition of EtOH to the residue, the resulting precipitate was collected by filtration, and washed with EtOH to give **17** (93.6 mg, 53%). ^1H NMR (DMSO−d_6) δ: 3.76 (s, 3H), 4.67 (dd, J = 5.5, 1.8 Hz, 1H), 4.94 (d, J = 5.4 Hz, 1H), 6.98 (d, J = 9.1 Hz, 2H), 7.33 (d, J = 8.5 Hz, 2H), 8.38 (br, 3H), 9.01 (s, 1H). MS (FI^+) *m/z*: 192 (M^+). HRMS (FI^+) for $C_{10}H_{12}N_2O_2$ (M^+): calcd, 192.08988; found, 192.09032. IR (ATR) cm^{-1}: 3078, 1752, 1728.

1-(4-Chlorophenyl)-3-[*cis*-2-(4-methoxyphenyl)-4-oxoazetidin-3-yl]urea (3). To a mixture of **17** (89.0 mg, 0.389 mmol), AcOEt (1.6 mL), and saturated aqueous $NaHCO_3$ solution was added 4-chlorophenyl isocyanate (56.0 mg, 0.365 mmol) under cooling with ice and the mixture was stirred at same temperature for 2 h. After quenching the reaction by the addition of water, the mixture was extracted with AcOEt (2 × 10 mL). The combined extracts were washed with brine, dried over anhydrous Na_2SO_4, filtered, and then concentrated in vacuo. Trituration of the residue with AcOEt−Et_2O gave **3** (85 mg, 63%) as a white powder. Mp: 184−186 ℃ ^{1}H NMR (DMSO−d_6) δ: 3.73 (s, 3H), 4.86 (d, J = 4.8 Hz, 1H), 5.29 (dd, J = 9.7, 4.8 Hz, 1H), 6.27 (d, J = 9.7 Hz, 1H), 6.93−6.97 (m, 2H), 7.13−7.16 (m, 2H), 7.22−7.25 (m, 2H), 7.28−7.31 (m, 2H), 8.49 (s, 1H), 8.61 (s, 1H). MS (FD$^+$) *m/z*: 345 (M$^+$). HRMS (FD$^+$) for $C_{17}H_{16}ClN_3O_3$ (M$^+$): calcd, 345.08802; found, 345.08767. IR (ATR) cm^{-1}: 3278, 1771, 1627. HPLC purity: 98.1%.

***trans*-3-Azide-1,2-*bis*(4-methoxyphenyl)azetidin-2-one (19).** To a mixture of **18** (530 mg, 1.77 mmol), triethylamine (0.37 mL, 2.7 mmol), and THF (8.9 mL) was added methanesulfonyl chloride (0.17 mL, 2.2 mmol) under cooling with ice; the mixture was stirred at same temperature for 1.5 h. After quenching the reaction by the addition of

ice−water, the mixture was extracted with CH_2Cl_2 (3 × 20 mL). The combined extracts were washed with brine, dried over anhydrous Na_2SO_4, filtered, and then concentrated in vacuo. A mixture of the residue, NaN_3 (690 mg, 10.6 mmol), and DMF (8.9 mL) was stirred at 90 °C for 74 h. After quenching the reaction by the addition of ice−water, the mixture was extracted with AcOEt (2 × 20 mL). The combined extracts were washed with brine, dried over anhydrous Na_2SO_4, filtered, and concentrated in vacuo. Flash chromatography (hexane/AcOEt = 3:1) of the residue gave **19** (510 mg, 89%) as a pale yellow solid. ^{1}H NMR ($CDCl_3$) δ: 3.74 (s, 3H), 3.81 (s, 3H), 4.46 (d, J = 1.8 Hz, 1H), 4.77 (d, J = 1.8 Hz, 1H), 6.76−6.80 (m, 2H), 6.90−6.93 (m, 2H), 7.19−7.23 (m, 2H), 7.24−7.28 (m, 2H). MS (ESI$^+$) *m/z*: 325 (M^+ + H). HRMS (ESI$^+$) for $C_{17}H_{17}N_4O_3$ (M^+ + H): calcd, 325.13006; found, 325.12938. IR (ATR) cm^{-1}: 2122, 1758.

***trans*-3-Azide-4-(4-methoxyphenyl)azetidin-2-one (20).** The compound **20** (285 mg, 85%) was prepared from **19** (500 mg, 1.54 mmol) by the same method as that used for **16**. ^{1}H NMR ($CDCl_3$) δ: 3.83 (s, 3H), 4.36 (d, J = 1.8 Hz, 1H), 4.55 (d, J = 1.8 Hz, 1H), 6.13 (br s, 1H), 6.92−6.95 (m, 2H), 7.27−7.30 (m, 2H). MS (FD$^+$) *m/z*: 218 (M^+). HRMS

(FD$^+$) for $C_{10}H_{10}N_4O_2$ (M^+): calcd, 218.08038; found, 218.08038. IR (ATR) cm^{-1}: 3079, 2101, 1772, 1733.

1-(4-Chlorophenyl)-3-[*trans*-2-(4-methoxyphenyl)-4-oxoazetidin-3-yl]urea (4). To a mixture of **20** (100 mg, 0.46 mmol) and THF (4.6 mL) was added triphenylphosphine (136 mg, 0.519 mmol), and the mixture was stirred at room temperature for 100 min. After addition of water (0.04 mL) to the resulting mixture, the reaction mixture was stirred at 50 °C for 5 h. To the resulting mixture was added 4-chlorophenyl isocyanate (48.0 mg, 0.31 mmo), and the mixture was stirred at room temperature for 70 min. To the resulting mixture was added 4-chlorophenyl isocyanate (15.0 mg, 0.098 mmo), and the mixture was stirred at room temperature for 10 min. After quenching the reaction by the addition of water, the mixture was extracted with AcOEt (2 × 10 mL). The combined extracts were washed with brine, dried over anhydrous Na_2SO_4, filtered, and concentrated in vacuo. Trituration of the residue with AcOEt−MeOH gave **4** (76.0 mg, 48%) as a white powder. Mp: 182−183 ℃. ^{1}H NMR (DMSO−d_6) δ: 3.75 (s, 3H), 4.37 (dd, J = 7.9, 2.4 Hz, 1H), 4.56 (d, J = 2.4 Hz, 1H), 6.93−6.97 (m, 2H), 7.01 (d, J = 7.9 Hz, 1H), 7.26−7.34 (m, 4H), 7.41−7.45 (m, 2H), 8.53 (s, 1H), 8.88 (s, 1H). MS (FD$^+$) *m/z*: 345 (M^+). HRMS (FD$^+$) for

$C_{17}H_{16}ClN_3O_3$ (M^+): calcd, 345.08802; found, 345.08802. IR (ATR) cm^{-1}: 3364, 1741, 1691. HPLC purity: 99.0%.

***tert*-Butyl 3-(4-Methoxyphenyl)-4-nitro-2-(2,2,2-trifluoroacetamido)butanoate (22).** Lithium *bis*(trimethylsilyl)amide (1.6 M THF solution, 44 mL, 70 mmol) was added dropwise to a solution of *tert*-butyl (2,2,2-trifluoroacetyl)glycinate (6.33 g, 27.9 mmol) in THF (50 mL) at -78 °C, and the mixture was stirred at same temperature for 30 min. To the resulting mixture was added dropwise a solution of **21** (5.00 g, 27.9 mmol) in THF (30 mL) at -78 °C, and then the mixture was stirred at room temperature for 30 min. After quenching the reaction by the addition of 1 M HCl, the mixture was extracted with AcOEt. The extract was washed with brine, dried over anhydrous Na_2SO_4, filtered, and concentrated in vacuo. Flash chromatography of the residue (hexane/AcOEt = 4:1) gave **22** (10.0 g, 88%)as a pale yellow oil. ^1H NMR ($CDCl_3$) δ: 1.38 and 1.47 [each s, total 9H, $C(CH_3)_3$ of major and minor isomers), 3.79 and 3.80 (each s, total 3H, OCH_3 of major and minor isomers), 3.96 (q, J = 7.3 Hz, 0.7H, C−3H of major isomer), 4.20−4.26 (m, 0.3H, C−3H of minor isomer), 4.63−4.69 (m, 0.3H, C−2H of minor isomer), 4.76−4.87 [m, 2H (C−4H of major and minor isomers)+0.7H (C−3H of major isomer)], 6.74−6.89 [m, 2H

(ArH of major and minor isomers)+1H (NH of major and minor isomers)], 7.05−7.10 (m, 2H, ArH of major and minor isomers).

3-(4-Methoxyphenyl)-4-nitro-2-(2,2,2-trifluoroacetamido)butanoic Acid (23). A mixture of **22** (10.0 g, 24.6 mmol) and trifluoroacetic acid (15 mL) was stirred at room temperature for 3 h and then concentrated in vacuo. A mixture of the resulting residue, AcOEt, and water was extracted with saturated aqueous $NaHCO_3$ solution. The aqueous layer was acidified with 1 M HCl, and then the mixture was extracted with AcOEt. The extract was washed with water and brine, dried over anhydrous Na_2SO_4, filtered, and then concentrated in vacuo to obtain **23** (5.0 g, 58%). Compound **23** was used for next step without further purification.

Methyl 3-(4-Methoxyphenyl)-4-nitro-2-(2,2,2-trifluoroacetamido)butanoate (24). To a solution of **23** (5.00 g, 14.3 mmol) in DMF (15 mL) was added $KHCO_3$ (2.86 g, 28.6 mmol) and iodomethane (1.78 mL, 28.6 mmol), and the mixture was stirred at 50 °C for 2 h. After quenching the reaction by the addition of water, the mixture was extracted with AcOEt. The extract was washed with water and brine, dried over anhydrous Na_2SO_4, filtered, and then concentrated in vacuo. Flash chromatography (hexane/AcOEt = 4:1)

of the residue gave **24** (4.8 g, 92%) as an off-white solid. ^{1}H NMR ($CDCl_3$) δ: 3.73 (s, 2H, OCH_3 of major isomer), 3.80 and 3.81 (each s, total 4H, OCH_3 of major and minor isomers), 4.00 (dd, J = 13.9, 7.9 Hz, 0.7H, C−3H of major isomer), 4.26−4.32 (m, 0.3H, C−3H of minor isomer), 4.68 (dd, J = 13.9, 8.5 Hz, 0.3H, C−4H of minor isomer), 4.85−4.94 [m, 2.1H (C−2H and C−4H of major isomer)+0.3H (C−2H of minor isomer], 5.01−5.07 (m, 0.3H, C−4H of minor isomer), 6.68−6.80 (br, 1H, NH of major and minor isomers), 6.88 (d J = 9.1 Hz, 2H, ArH of major and minor isomers), 7.00−7.03 (m, 2H, ArH of major and minor isomers). MS (FI$^+$) *m/z*: 364 (M^+). HRMS (FI$^+$) for $C_{14}H_{15}F_3N_2O_6$ (M^+): calcd, 364.08822; found, 364.08839. IR (ATR) cm^{-1}: 3266, 1734, 1706.

2,2,2-Trifluoro-*N*-[4-(4-methoxyphenyl)-2-oxopyrrolidin-3-yl]acetamide (25). To a solution of **24** (4.78 g, 13.1 mmol) in MeOH (130 mL) were added a solution of NH_4Cl (7.00 g, 131 mmol) in water (30 mL) and zinc powder (8.50 g, 131 mmol), and the mixture was stirred at room temperature for 30 min. The reaction mixture was diluted with AcOEt and the insoluble materials were filtered off. After addition of saturated aqueous $NaHCO_3$ solution to the filtrate, the mixture was extracted with AcOEt. The extract was washed with water and brine, dried over anhydrous Na_2SO_4, filtered, and then concentrated in

vacuo. To a solution of the residue in MeOH (65 mL) was added a solution of sodium acetate (13.0 g, 159 mmol) in water (43 mL) and 20% aqueous titanium(III) chloride solution (17 mL), and then the mixture was stirred at room temperature for 2 h. After quenching the reaction by additioon of water, the mixture was extracted with AcOEt. The extract was washed with water and brine, dried over anhydrous Na_2SO_4, filtered, and then concentrated in vacuo. Flash chromatography (hexane/AcOEt = 1:2) of the residue gave **25** (2.5 g, 63%) as a pale yellow oil. ^{1}H NMR ($CDCl_3$) δ: 3.43 (t, J = 9.7 Hz, 0.3H, C−5H of minor isomer), 3.61−3.68 (m, 1H, C−5H of major and minor isomers), 3.73 (t, J = 9.7 Hz, 0.3H, C−4H of minor isomer), 3.79 and 3.81 (each s, total 3H, OCH_3 of major and minor isomers), 3.93 (dd, J = 10.3, 6.7 Hz, 0.7H, C−5H of major isomer), 4.04 (t, J = 6.7 Hz, 0.7H, C−4H of major isomer), 4.72 (dd, J = 10.9, 8.5 Hz, 0.3H, C−3H of minor isomer), 4.77 (t, J = 6.7 Hz, 0.7H, C−3H of major isomer), 6.31 (br s, 1H, NH of major and minor isomers), 6.34−6.42 (br, 0.7H, NH of major isomer), 6.84 (d, J = 9.1 Hz, 1.3H, ArH of major isomer), 6.91 (d, J = 8.5 Hz, 0.7H, ArH of minor isomer), 7.00 (d, J = 7.9 Hz, 0.3H, NH of minor isomer), 7.07 (d, J = 8.5 Hz, 1.3H, ArH of major isomer), 7.22 (d, J = 8.5 Hz,

0.7H, ArH of minor isomer). MS (FI$^+$) *m/z*: 302 (M$^+$). HRMS (FI$^+$) for $C_{13}H_{13}F_3N_2O_3$ (M$^+$): calcd, 302.08783; found, 302.08781. IR (ATR) cm^{-1}: 3296, 3235, 1722, 1696, 1674.

1-(4-Chlorophenyl)-3-[*cis*-4-(4-methoxyphenyl)-2-oxopyrrolidin-3-yl]urea (5) and 1-(4-Chlorophenyl)-3-[*trans*-4-(4-methoxyphenyl)-2-oxopyrrolidin-3-yl]urea (6). To a solution of **25** (60.0 mg, 0.199 mmol) in MeOH (3.0 mL) was added 1 M aqueous NaOH solution (0.5 mL), and the mixture was stirred at 70 °C for 2 h. After neutralization (pH 7) of the reaction mixture by addition of 1 M HCl, the mixture was concentrated in vacuo. To the mixture of residue (**26**) and AcOEt (3.0 mL), 4-chlorophenyl isocyanate (30.0 mg, 0.195 mmol) was added, and the mixture was stirred at room temperature for 10 min. After dilution of the reaction mixture with AcOEt, the mixture was washed with water and brine, dried over anhydrous Na_2SO_4, filtered, and concentrated in vacuo. Flash chromatography (hexne/AcOEt → AcOEt → AcOEt/MeOH) of the residue gave **5** (3.00 mg, 4.2%) and **6** (31.0 mg, 44%).

26: ^{1}H NMR ($CDCl_3$) δ: 3.20−3.27 (m, 1H), 3.36 (d, J = 9.7 Hz, 1H), 3.58−3.74 (m, 2H), 3.81 (s, 3H), 5.91 (br s, 1H), 6.86−6.92 (m, 2H), 7.17−7.24 (m, 2H). MS (FI$^+$) *m/z*: 206 (M$^+$). HRMS (FI$^+$) for $C_{11}H_{14}N_2O_2$ (M$^+$): calcd, 206.10553; found, 206.10598.

5.: White powder. Mp: 211−213 ℃. ^{1}H NMR (DMSO−d_6) δ: 3.25−3.30 (m, 1H), 3.68−3.72 (m, 5H), 4.59 (t, J = 7.3 Hz, 1H), 5.80 (d, J = 7.3 Hz, 1H), 6.83−6.87 (m, 2H), 7.03−7.06 (m, 2H), 7.21−7.25 (m, 2H), 7.30−7.34 (m, 2H), 8.10 (s, 1H), 8.73 (s, 1H). MS (ESI$^+$) *m/z*: 360 (M^+ + H). HRMS (ESI$^+$) for $C_{18}H_{19}ClN_3O_3$ (M^+ + H): calcd, 360.11149; found, 360.11120. IR (ATR) cm^{-1}: 3303, 1699. HPLC purity: 99.0%.

6.: White powder. Mp: 151−154 ℃. ^{1}H NMR (DMSO−d_6) δ: 3.13−3.20 (m, 1H), 3.43−3.50 (m, 2H), 3.72 (s, 3H), 4.48 (dd, J = 10.9, 9.1 Hz, 1H), 6.47 (d, J = 8.5 Hz, 1H), 6.86−6.90 (m, 2H), 7.22−7.26 (m, 2H), 7.28−7.32 (m, 2H), 7.37−7.41 (m, 2H), 7.92 (s, 1H), 8.68 (s, 1H). MS (ESI$^+$) *m/z*: 360 (M^+ + H). HRMS (ESI$^+$) for $C_{18}H_{19}ClN_3O_3$ (M^+ + H): calcd, 360.11149; found, 360.11142. IR (ATR) cm^{-1}: 3387, 1729, 1660. HPLC purity: 99.0%.

Dimethyl 2-[2-Cyano-1-(4-methoxyphenyl)ethyl]malonate (28). To a 1 M soluion of sodium methoxide in MeOH [prepared from sodium (460 mg, 20.0 mmol) and MeOH (20 mL)] was added dimethyl malonate (3.00 mL, 26.3 mmol), and the mixture was stirred at room temperature for 10 min. To the reaction mixture was added **27** (2.90 mL, 20.0 mmol), and the mixture was heated under reflux for 18 h. After quenching the reaction

by the addition of 1 M HCl (50 mL) under ice cooling, the mixture was extracted with AcOEt (2 × 100 mL). The combined extracts were washed with brine (2 × 50 mL), dried over anhydrous Na_2SO_4, filtered, and concentrated in vacuo. After susupension of the residue in MeOH (50 mL), the insoluble materials were filtered off, and the filtrate was concentrated in vacuo. Flash chromatography (hexane/AcOEt = 10:1 → 1:2) of the residue gave **28** (1.43 g, 24%) as a white solid. ^{1}H NMR ($CDCl_3$) δ: 2.83 (dd, J = 17.0, 4.8 Hz, 1H), 2.89 (dd, J = 16.3, 7.3 Hz, 1H), 3.53 (s, 3H), 3.67−3.73 (m, 1H), 3.786 (s, 3H), 3.795 (s, 3H), 3.85 (d, J = 9.7 Hz, 1H), 6.85−6.89 (m, 2H), 7.18−7.22 (m, 2H). MS (EI$^+$) *m/z*: 291 (M^+). IR (ATR) cm^{-1}: 2248, 1750, 1734.

Methyl 4-(4-Methoxyphenyl)-2-oxopiperidine-3-carboxylate (29). To a mixture of **28** (1.31 g, 4.50 mmol) and nickel(II) chloride hexahydrate (1.07 g, 4.50 mmol) in MeOH (45 mL) was added portionwise $NaBH_4$ (1.02 g, 27.0 mmol) under cooling with ice, and the mixture was stirred at room temperature for 1 h. After quenching the reaction by adding 1 M HCl (30 mL), the mixture was extracted with AcOEt (2 × 100 mL). The combined extracts were washed with water and brine, dried over anhydrous Na_2SO_4, filtered, and concentrated in vacuo. Flash chromatography (hexane/AcOEt = 1:2) of the residue gave

29 (765 mg, 65%) as a white solid. ^{1}H NMR (DMSO−d_6) δ: 1.80 (br d, J = 13.5 Hz, 1H), 1.97 (dq, J = 12.7, 5.5 Hz, 1H), 3.14−3.31 (m, 3H), 3.44 (s, 3H), 3.52 (d, J = 11.5 Hz, 1H), 3.72 (s, 3H), 6.84−6.87 (m, 2H), 7.16−7.19 (m, 2H), 7.89 (d, J = 2.4 Hz, 1H). MS (ESI$^+$) *m/z*: 264 (M^+ + H). IR (ATR) cm^{-1}: 3191, 1740, 1656.

4-(4-Methoxyphenyl)-2-oxopiperidine-3-carboxylic Acid (30). To a solution of **29** (710 mg, 2.70 mmol) in MeOH (5.4 mL) was added 1 M aqueous NaOH solution (5.40 mL, 5.40 mmol) and then the mixture was stirred at 50 °C for 1 h. After removal of MeOH in vacuo, the resulting mixture was adjusted to pH 1 by addition of 1 M HCl under cooling with ice, and the resulting precipitate was collected by filtration. The filtered precipitate was washed with water and hexane, and dried in vacuo to give **30** (618 mg, 92%) as a white solid. ^{1}H NMR (DMSO−d_6) δ: 1.79 (br d, J = 13.3 Hz, 1H), 1.92 (dq, J = 12.7, 5.5 Hz, 1H), 3.11−3.30 (m, 3H), 3.36 (d, J = 11.5 Hz, 1H), 3.72 (s, 3H), 6.84−6.68 (m, 2H), 7.17−7.21 (m, 2H), 7.80 (d, J = 3.0 Hz, 1H), 12.2 (br s, 1H). MS (FD$^+$) *m/z*: 249 (M^+). IR (ATR) cm^{-1}: 3305, 1740.

1-(4-Chlorophenyl)-3-[*trans*-4-(4-methoxyphenyl)-2-oxopiperidin-3-yl]urea (7). Diphenylphosphoryl azide (0.17 mL, 0.760 mmol) and triethylamine (0.11 mL, 0.789

mmol) were added to a mixture of **30** (150 mg, 0.602 mmol) in toluene (3.0 mL) and MeCN (0.3 mL), the mixture was stirred at room temperature for 1 h, and then at 100 °C for 1 h. To the reaction mixture was added 4-chloroaniline (155 mg, 1.22 mmol), the mixture was stirred at 100 °C for 6.5 h, and concentrated in vacuo. Flash chromatography (AcOEt → AcOEt/MeOH = 4:1) of the residue gave **7** (14.6 mg, 6.5%) as a white powder. Mp: 254−260 ℃. ^{1}H NMR (DMSO−d_6) δ: 1.85 (br d, J = 12.1 Hz, 1H), 2.01 (dq, J = 12.1, 5.5 Hz, 1H), 3.12−3.21 (m, 2H), 3.26 (dt, J = 11.5, 4.2 Hz, 1H), 3.69 (s, 3H), 4.13 (dd, J = 11.5, 9.1 Hz, 1H), 6.24 (d, J = 9.1 Hz, 1H), 6.82 (d, J = 8.5 Hz, 2H), 7.17 (d, J = 8.5 Hz, 2H), 7.20 (d, J = 9.1 Hz, 2H), 7.34 (d, J = 9.1 Hz, 2H), 7.61 (s, 1H), 8.59 (s, 1H). MS (ESI$^+$) *m/z*: 374 (M^+ + H). HRMS (ESI$^+$) for $C_{19}H_{21}ClN_3O_3$ (M^+ + H): calcd, 374.12714; found, 374.12805. IR (ATR) cm^{-1}: 3322, 1678, 1647. Anal calcd for $C_{19}H_{20}ClN_3O_3 \cdot 0.8H_2O$: C, 58.78; H, 5.61; N, 10.82. Found: C, 58.84; H, 5.34; N, 10.74.

Ethyl 2-[(*tert*-butoxycarbonyl)amino]-3-(4-methoxyphenyl)-4-nitrobutanoate (31). Lithium diisopropylamide (1.09 M THF solution, 18.3 mL, 20.0 mmol) was added dropwise to a solution of ethyl 2-[(diphenylmethylene)amino]acetate (5.35 g, 20.0 mmol) in THF (56 mL) at -78 °C, and the mixture was stirred at -78 °C for 1 h. To the reaction mixture was

added dropwise a solution of **21** (3.00 g, 16.7 mmol) in THF (16 mL) at -78 °C, and the mixture was stirred for 4.5 h with gradually warming to room temperature. The reaction mixture was poured into saturated aqueous NH_4Cl solution (150 mL), and the resulting mixture was extracted with AcOEt (2 × 30 mL). The combined extracts were washed with brine, dried over anhydrous Na_2SO_4, filtered, and then concentrated in vacuo. Flash chromatography (hexane/AcOEt = 4:1) of the residue gave ethyl 2-[(diphenylmethylene)amino]-3-(4-methoxyphenyl)-4-nitrobutanoate (8.47 g). A mixture of the compound obtained (8.47 g), acetic acid (45 mL) and water (9 mL) was stirred at 45 °C for 4 h, and then at 50 °C for 2 h. After addition of 0.5 M HCl (70 mL) and diethyl ether (20 mL) to the reaction mixture, the aqueous layer was separated and washed with diethyl ether (2 × 20 mL). The resulting mixture was neutralized with saturated aqueous $NaHCO_3$ solution, and extracted with AcOEt (2 × 50 mL). The combined extracts were washed with brine, dried over anhydrous Na_2SO_4, filtered, and concentrated in vacuo. Di-*tert*-butyl dicarbonate (4.02 g, 18.4 mmol) and THF (42 mL) were added to the residue and the reaction mixture was stirred at room temperature for 6 h. To the reaction mixture were added AcOEt (30 mL) and water (100 mL). The organic layer was separated and the

aqueous layer was extracted with AcOEt (2 × 20 mL). The combined extracts were washed with brine, dried over anhydrous Na_2SO_4, filtered, and concentrated in vacuo. Flash chromatography (hexane/AcOEt = 95:5 → 4:1) of the residue gave **31** (4.00 g, 63%). ^{1}H NMR ($CDCl_3$) δ: 1.08 (br, 3H), 1.46 (s, 9H), 3.78 (s, 3H), 3.79−3.85 (m, 1H), 4.01 (d, J = 6.7 Hz, 2H) , 4.53−4.57 (m, 1H), 4.77 (dd, J = 13.4 Hz, 9.2 Hz, 1H), 4.85 (dd, J = 13.4 Hz, 5.5 Hz, 1H), 5.11 (br, 1H), 6.85 (d, J = 8.6 Hz, 2H), 7.10 (d, J = 8.6 Hz, 2H). MS (ESI$^+$) *m/z*: 383 (M^+ + H). HRMS (ESI$^+$) for $C_{18}H_{27}N_2O_7$ (M^+ + H): calcd, 383.18183; found, 383.18131. IR (ATR) cm^{-1}: 3401, 1732, 1697.

(-)-*tert*-Butyl [4-(4-methoxyphenyl)-2-oxopyrrolidin-3-yl]carbamate (32) and (+)-*tert*-Butyl [4-(4-methoxyphenyl)-2-oxopyrrolidin-3-yl]carbamate (33). To a mixture of **31** (4.00 g, 10.5 mmol) and nickel(II) chloride hexahydrate (2.50 g, 10.5 mmol) in MeOH (210 mL) was added portionwise $NaBH_4$ (2.38 g, 63.0 mmol) under cooling with ice, the mixture was stirred at room temperature for 45 min, and then at 40 °C for 2 h. The reaction mixture was poured into saturated aqueous NH_4Cl solution, and the resulting mixture was extracted with AcOEt (500 mL). The extract was washed with brine, dried over anhydrous Na_2SO_4, filtered, and then concentrated in vacuo. Flash chromatography (hexane/AcOEt

= 3:2) of the residue gave the racematic *tert*-butyl [4-(4-methoxyphenyl)-2-oxopyrrolidin-3-yl]carbamate (2.68 g). Chiral separation of the racemate by HPLC using CHIRALPAK AD column (hexane/EtOH/*tert*-butyl methyl ether =45:30:25) gave **32** (1.14 g, 35%) and **33** (1.40 g, 43%).

32. ^{1}H NMR ($CDCl_3$) δ: 1.37 (s, 9H), 3.55 (d, J = 9.8 Hz, 1H), 3.80 (s, 3H), 3.82−3.92 (m, 2H), 4.58 (br s, 2H), 5.75 (br s, 1H), 6.83 (d, J = 8.6 Hz, 2H), 7.10 (d, J = 8.6 Hz, 2H). MS (ESI$^+$) *m/z*: 307 (M^+ + H). HRMS (ESI$^+$) for $C_{16}H_{23}N_2O_4$ (M^+ + H): calcd, 307.16578; found, 307.16561. IR (ATR) cm^{-1}: 3363, 3287, 1708, 1684. $[\alpha]^{22}_D$ −88.2 (*c* 0.104, EtOH).

33. ^{1}H NMR ($CDCl_3$) δ: 1.37 (s, 9H), 3.56 (d, J = 9.8 Hz, 1H), 3.80 (s, 3H), 3.82−3.97 (m, 2H), 4.58 (br s, 2H), 5.73 (br s, 1H), 6.83 (d, J = 8.6 Hz, 2H), 7.10 (d, J = 8.6 Hz, 2H). MS (ESI$^+$) *m/z*: 307 (M^+ + H). HRMS (ESI$^+$) for $C_{16}H_{23}N_2O_4$ (M^+ + H): calcd, 307.16578; found, 307.16615. IR (ATR) cm^{-1}: 3363, 3287, 1708, 1684. $[\alpha]^{22}_D$ +98.4 (*c* 0.101, EtOH).

(-)-1-(4-Chlorophenyl)-3-[*cis*-4-(4-methoxyphenyl)-2-oxopyrrolidin-3-yl]urea (8). Trifluoroacetic acid (0.5 mL) was added to a solution of **32** (42.9 mg, 0.140 mmol) in CH_2Cl_2 (1 mL) at 0 °C, and the mixture was stirred at room temperature for 75 min. After concentration of the reaction mixture in vacuo, a mixture of the residue, saturated

aqueous $NaHCO_3$, THF (1 mL), and 4-chlorophenyl isocyanate (23.6 mg, 0.154 mmol) was stirred at room temperature for 1 h. To the reaction mixture was added 4-chlorophenyl isocyanate (11 mg, 0.070 mmol), and the mixture was stirred at room temperature for 40 min, and concentrated in vacuo. Flash chromatography of the residue ($CHCl_3$/MeOH = 10:1) gave **8** (28.0 mg, 56%) as a white powder. Mp: 212−214 ℃. ^{1}H NMR (DMSO−d_6) δ: 3.25−3.31 (m, 1H), 3.68−3.72 (m, 5H), 4.59 (t, J = 7.3 Hz, 1H), 5.81 (d, J = 6.7 Hz, 1H), 6.83−6.87 (m, 2H), 7.03−7.06 (m, 2H), 7.21−7.25 (m, 2H), 7.30−7.34 (m, 2H), 8.10 (s, 1H), 8.74 (s, 1H). MS (ESI$^+$) *m/z*: 360 (M^+ + H). HRMS (ESI$^+$) for $C_{18}H_{19}ClN_3O_3$ (M^+ + H): calcd, 360.11149; found, 360.11194. IR (ATR) cm^{-1}: 3301, 1664. Enantiomeric excess was determined by HPLC analysis with CHIRALPAK ID column (30:70 hexane:EtOH, 1.0 mL/mim, 254 nm); major enantiomer t_r = 11.2 min; 100% ee; $[\alpha]^{25}_D$ -260 (*c* 0.101, EtOH). HPLC purity 100%

(+)-1-(4-Chlorophenyl)-3-[*cis*-4-(4-methoxyphenyl)-2-oxopyrrolidin-3-yl]urea (9). The compound **9** (26.6 mg, 56%) was prepared from **33** (40.3 mg, 0.132 mmol) by the same method as that used for **8**. White powder. Mp: 211−214 ℃. ^{1}H NMR (DMSO−d_6) δ: 3.25−3.31 (m, 1H), 3.68−3.72 (m, 5H), 4.59 (t, J = 7.3 Hz, 1H), 5.81 (d, J = 7.3 Hz, 1H),

6.83−6.87 (m, 2H), 7.03−7.06 (m, 2H), 7.21−7.25 (m, 2H), 7.30−7.34 (m, 2H), 8.10 (s, 1H), 8.74 (s, 1H). MS (ESI$^+$) *m/z*: 360 (M$^+$ + H). HRMS (ESI$^+$) for $C_{18}H_{19}ClN_3O_3$ (M$^+$ + H): calcd, 360.11149; found, 360.11186. IR (ATR) cm^{-1}: 3304, 1684, 1666. Enantiomeric excess was determined by HPLC analysis with CHIRALPAK ID column (30:70 hexane:EtOH, 1.0 mL/mim, 254 nm); major enantiomer t_r = 12.5 min; 100% ee; $[\alpha]^{25}_D$ +235 (*c* 0.104, EtOH). HPLC purity 99.9%.

Methyl (3*R*,4*S*)-4-(4-Methoxyphenyl)-2-oxopyrrolidine-3-carboxylate (35). To a solution of **21** (12.0 g, 64.3 mmol) in toluene (64 mL) was added dimethyl malonate (7.50 mL, 64.3 mmol) and nickel(II)-*bis*[(*R*,*R*)-*N*,*N*-dibenzylcyclohexan-1,2-diamine]bromide (1.56 g, 1.93 mmol), and the mixture was stirred at room temperature for 28 h. The reaction mixture was washed with 0.1 M HCl (50 mL) and water (50 mL), dried over anhydrous Na_2SO_4, filtered, and then concentrated in vacuo to give dimethyl (*S*)-2-[1-(4-methoxyphenyl)-2-nitroethyl]malonate (**34**) as a white solid. To a mixture of crude **34** and nickel(II) chloride hexahydrate (17.2 g, 70.7 mmol) in MeOH (322 mL) was added portionwise $NaBH_4$ (14.9 g, 386 mmol) under cooling with ice, and then the mixture was stirred at room temperature for 2.5 h. To the reaction mixture was added saturated

aqueous NH_4Cl (800 mL) and AcOEt (1200 mL) under cooling with ice, and the mixture was stirred at room temperature for 2 h, and then the organic layer was separated. The organic layer was washed with saturated aqueous NH_4Cl (500 mL), water (500 mL), and brine (500 mL), dried over anhydrous Na_2SO_4, filtered, and concentrated in vacuo. Trituration of the residue with EtOH−diisopropyl ether gave **35** (11.6 g, 73%) as a white solid.

34. ^{1}H NMR ($CDCl_3$) δ: 3.58 (s, 3H), 3.76 (s, 3H), 3.78 (s, 3H), 3.83 (d, J = 9.1 Hz, 1H), 4.19 (dt, J = 9.1, 4.8 Hz, 1H), 4.83 (dd, J = 12.7, 9.1 Hz, 1H), 4.89(dd, J = 12.7, 4.8 Hz, 1H), 6.82−6.86 (m, 2H), 7.13−7.16 (m, 2H). Enantiomeric excess was determined by HPLC analysis with CHIRALPAK ID column (90:10 hexane:EtOH, 1.0 mL/mim, 254 nm); minor enantiomer t_r = 21.5 min, major enantiomer t_r = 19.8 min; 92.4% ee; $[\alpha]^{25}_D$ +5.33 (c 1.121, $CHCl_3$).

35. ^{1}H NMR ($CDCl_3$) δ: 3.40 (t, J = 8.5 Hz, 1H), 3.54 (d, J = 9.7 Hz, 1H), 3.71−3.74 (m, 1H), 3.78 (s, 3H), 3.80 (s, 3H), 4.09 (q, J = 8.5 Hz, 1H), 5,72 (br s, 1H), 6.86−6.90 (m, 2H), 7.17−7.20 (m, 2H). MS (FI$^+$) *m/z*: 249 (M^+). HRMS (FI$^+$) for $C_{13}H_{15}NO_4$ (M^+): calcd, 249.10011; found, 249.10051. IR (ATR) cm^{-1}: 3226, 1718, 1693. Enantiomeric excess

was determined by HPLC analysis with CHIRALPAK ID column (80:20 hexane:EtOH, 1.0 mL/mim, 254 nm); minor enantiomer t_r = 14.4 min, major enantiomer t_r = 17.0 min; 99.1% ee; $[\alpha]^{25}_D$ +154 (*c* 0.164, EtOH).

(3*R*,4*S*)-4-(4-Methoxyphenyl)-2-oxopyrrolidine-3-carboxylic Acid (36). To a solution of **35** (200 mg, 0.802 mmol) in MeOH (4.0 mL) was added 2 M NaOH solution (0.80 mL, 1.6 mmol), and the mixture was stirred at 60 °C for 1.5 h. After addition of 1 M HCl (1.8 mL) to the reaction mixture, water (25 mL) was added, and the mixture was extracted with AcOEt (2 × 35 mL). The combined extracts were washed with brine, dried over anhydrous Na_2SO_4, filtered, and concentrated in vacuo to give **36** (166 mg, 88%). ^{1}H NMR (DMSO−d_6) δ: 3.16 (t, J = 9.1 Hz, 1H), 3.41 (br d, 1H), 3.55 (t, J = 8.5 Hz, 1H), 3.72 (s, 3H), 3.79 (q, J = 8.5 Hz, 1H), 6.88 (d, J = 8.5 Hz, 2H), 7.24 (d, J = 8.5 Hz, 2H), 8.01 (s, 1H), 12.6 (br s, 1H). MS (FD$^+$) *m/z*: 235 (M^+). HRMS (FD$^+$) for $C_{12}H_{13}NO_4$ (M^+): calcd, 235.08446; found, 235.08379. IR (ATR) cm^{-1}: 3239, 1686. $[\alpha]^{25}_D$ +146 (*c* 0.192, EtOH).

1-(4-Chlorophenyl)-3-[(3*R*,4*S*)-4-(4-methoxyphenyl)-2-oxopyrrolidin-3-yl]urea (10). To a mixture of **36** (80.0 mg, 0.340 mmol) in toluene (1.7 mL) was added triethylamine (61.9 µL, 0.442 mmol) and diphenyphosphoryl azide (80.6 µL, 0.374 mmol), and the mixture

was stirred at room temperature for 4.5 h and then at 60 °C for 45 min. To the reaction mixture was added 4-chloroaniline (87.6 μL, 0.680 mmol), and the mixture was stirred at 90 °C for 2.5 h. AcOEt (3.0 mL) and 1 mol/L HCl (2.0 mL) were added to the reaction mixture and the organic layer was separated. The organic layer was washed with 1 M HCl, saturated aqueous $NaHCO_3$ solution, and brine, dried over anhydrous Na_2SO_4, filtered, and concentrated in vacuo. Flash chromatography (AcOEt → AcOEt/MeOH = 20:1) of the residue gave **10** (65 mg, 53%) as a white powder. Mp: 191−193 ℃. ^{1}H NMR (DMSO−d_6) δ: 3.13−3.20 (m, 1H), 3.42−3.50 (m, 2H), 3.72 (s, 3H), 4.47 (dd, J = 10.9, 9.1 Hz, 1H), 6.49 (d, J = 9.1 Hz, 1H), 6.86−6.90 (m, 2H), 7.22−7.26 (m, 2H), 7.28−7.32 (m, 2H), 7.37−7.41 (m, 2H), 7.92 (s, 1H), 8.70 (s, 1H). MS (ESI$^+$) *m/z*: 360 (M^+ + H). HRMS (ESI$^+$) for $C_{18}H_{19}ClN_3O_3$ (M^+ + H): calcd, 360.11149; found, 360.11120. IR (ATR) cm^{-1}: 3303, 1664. Enantiomeric excess was determined by HPLC analysis with CHIRALPAK ID column (50:50 hexane:EtOH, 1.0 mL/mim, 254 nm); minor enantiomer t_r = 7.1 min, major enantiomer t_r = 11.0 min; 99.9% ee; $[\alpha]^{25}_D$ +145 (*c* 0.298, EtOH). HPLC purity 99.5%.

Methyl (3*S*,4*R*)-4-(4-Methoxyphenyl)-2-oxopyrrolidine-3-carboxylate (38). Compound **38** (19.2 g, 68%) was prepared from **21** (20.0 g, 112 mmol) and nickel(II)-*bis*[(*S*,*S*)-*N*,*N*-dibenzylcyclohexan-1,2-diamine]bromide (2.56 g, 3.28 mmol) by the same method as that used for **35**.

37. White solid. ^{1}H NMR ($CDCl_3$) δ: 3.57 (s, 3H), 3.76 (s, 3H), 3.78 (s, 3H), 3.83 (d, J = 9.1 Hz, 1H), 4.19 (d t, J = 9.1, 5.4 Hz, 1H), 4.82 (dd, J = 13.3, 9.1 Hz, 1H), 4.89 (dd, J = 13.3, 5.5 Hz, 1H), 6.82−6.86 (m, 2H), 7.12−7.16 (m, 2H). Enantiomeric excess was determined by HPLC analysis with CHIRALPAK ID column (90:10 hexane:EtOH, 1.0 mL/mim, 254 nm); minor enantiomer t_r = 20.4 min, major enantiomer t_r = 21.9 min; 92.5% ee; $[\alpha]^{25}_D$ −7.25 (*c* 1.230, $CHCl_3$).

38. Pale brown solid. ^{1}H NMR ($CDCl_3$) δ: 3.40 (t, J = 9.1 Hz, 1H), 3.54 (d, J = 10.3 Hz, 1H), 3.76−3.80 (s × 2 + m, total 7H), 4.09 (q, J = 8.5 Hz, 1H), 5,75 (br s, 1H), 6.86−6.90 (m, 2H), 7.17−7.20 (m, 2H). MS (FI$^+$) *m/z*: 249 (M^+). HRMS (FI$^+$) for $C_{13}H_{15}NO_4$ (M^+): calcd, 249.10011; found, 249.09991. IR (ATR) cm^{-1}: 3226, 1738, 1718, 1692. Enantiomeric excess was determined by HPLC analysis with CHIRALPAK ID column

(80:20 hexane:EtOH, 1.0 mL/mim, 254 nm); minor enantiomer t_r = 16.3 min, major enantiomer t_r = 13.6 min; 99.1% ee; $[\alpha]^{25}_D$ −145 (*c* 0.187, EtOH).

(3*S*,4*R*)-4-(4-Methoxyphenyl)-2-oxopyrrolidine-3-carboxylic Acid (39). Compound **39** (1.85 g, 98%) was prepared from **38** (2.00 g, 8.02 mmol) by the same method as that used for **36**. Pale brown solid. ^{1}H NMR (DMSO−d_6) δ: 3.16 (t, J = 9.1 Hz, 1H), 3.42 (d, J = 10.9 Hz, 1H), 3.55 (t, J = 8.5 Hz, 1H), 3.72 (s, 3H), 3.79 (q, J = 9.1 Hz, 1H), 6.88 (d, J = 8.5 Hz, 2H), 7.24 (d, J = 9.1 Hz, 2H), 8.03 (s, 1H), 12.5 (br s, 1H). MS (ESI$^+$) *m/z*: 236 (M^+ + H). HRMS (ESI$^+$) for $C_{12}H_{14}NO_4$ (M^+ + H): calcd, 236.09228; found, 236.09242. IR (ATR) cm^{-1}: 3240, 1686. $[\alpha]^{26}_D$ −139 (*c* 0.148, EtOH).

1-(4-Chlorophenyl)-3-[(3*S*,4*R*)-4-(4-methoxyphenyl)-2-oxopyrrolidin-3-yl]urea (11a). Compound **11a** (40 mg, 24%) was prepared from **39** (110 mg, 0.47 mmol) by the same method as that used for **10**. White powder. Mp: 192−195 °C. ^{1}H NMR (DMSO−d_6) δ: 3.13−3.20 (m, 1H), 3.43−3.50 (m, 2H), 3.72 (s, 3H), 4.48 (dd, J = 10.9, 9.1 Hz, 1H), 6.47 (d, J = 9.1 Hz, 1H), 6.86−6.90 (m, 2H), 7.22−7.26 (m, 2H), 7.28−7.32 (m, 2H), 7.37−7.41 (m, 2H), 7.92 (s, 1H), 8.68 (s, 1H). MS (ESI$^+$) *m/z*: 360 (M^+ + H). HRMS (ESI$^+$) for $C_{18}H_{19}ClN_3O_3$ (M^+ + H): calcd, 360.11149; found, 360.11076. IR (ATR) cm^{-1}: 3333, 1669.

Enantiomeric excess was determined by HPLC analysis with CHIRALPAK ID column (50:50 hexane:EtOH, 1.0 mL/mim, 254 nm); minor enantiomer t_r = 11.1 min, major enantiomer t_r = 7.1 min; 99.7% ee; $[\alpha]^{28}_D$ −130 (*c* 0.101, EtOH). HPLC purity 97.4%.

1-(4-Fluorophenyl)-3-[(3*S*,4*R*)-4-(4-methoxyphenyl)-2-oxopyrrolidin-3-yl]urea (11b). Compound **11b** (44 mg, 18%) was prepared from **39** (170 mg, 0.773 mmol) and 4-fluoroaniline (140 µL, 1.45 mmol) by the same method as that used for **10**. White powder. Mp: 203−204 °C. ^{1}H NMR (DMSO−d_6) δ: 3.13−3.20 (m, 1H), 3.42−3.50 (m, 2H), 3.72 (s, 3H), 4.47 (dd, *J* = 10.9, 9.1 Hz, 1H), 6.41 (d, *J* = 8.5 Hz, 1H), 6.86−6.90 (m, 2H), 7.01−7.07 (m, 2H), 7.28−7.32 (m, 2H), 7.33−7.39 (m, 2H), 7.91 (s, 1H), 8.55 (s, 1H). MS (ESI$^+$) *m/z*: 344 (M^+ + H). HRMS (ESI$^+$) for $C_{18}H_{19}FN_3O_3$ (M^+ + H): calcd, 344.14104; found, 344.14061. IR (ATR) cm^{-1}: 3345, 1673. $[\alpha]^{28}_D$ −156 (*c* 0.100, EtOH). HPLC purity: 99.6%.

(*E*)-2.6-Difluoro-4-methoxyl-(2-nitrovinyl)benzene (41). Ammonium acetate (11.2 g, 145 mmol) and nitromethane (22.9 mL, 427 mmol) were added to a solution of **40** (14.7 g, 85.4 mmol) in acetic acid (85 mL), the mixture was stirred at 100 °C for 6 h, and concentrated in vacuo. Water (50 mL) was added to the residue and the resulting precipitates were collected by filtration. The precipitates were washed with water and dried in vacuo to give **41** (17.5 g, 95%) as a yellow solid. ^{1}H NMR ($CDCl_3$) δ: 3.87 (s, 3H), 6.56 (d, *J* = 10.3 Hz, 2H), 7.77 (d, *J* = 13.9 Hz, 1H), 8.11 (d, *J*

= 13.9 Hz, 1H). MS (EI^+) *m/z*: 215 (M^+). HRMS (EI^+) for $C_9H_7F_2NO_3$ (M^+): calcd, 215.03940; found, 215.03889. IR (ATR) cm^{-1}: 1624, 1571, 1509.

Dimethyl (*R*)-[1-(2,6-Difluoro-4-methoxyphenyl)-2-nitroethyl]malonate (42). Compound **42** (22.5 g, 95%) was prepared from **41** (14.7 g, 68.3 mmol) by the same method as that used for **37**. White solid. ^1H NMR ($CDCl_3$) δ: 3.57 (s, 3H), 3.77 (s, 3H), 3.80 (s, 3H), 3.92 (d, J = 10.4 Hz, 1H), 4.66 (dt, J = 9.8, 4.9 Hz, 1H), 4.81 (dd, J = 12.8, 9.8 Hz, 1H), 4.91 (dd, J = 12.8, 4.9 Hz, 1H), 6.41−6.47 (m, 2H). MS (FI^+) *m/z*: 347 (M^+). HRMS (FI^+) for $C_{14}H_{15}F_2NO_7$ (M^+): calcd, 347.08166; found, 347.082160. IR (ATR) cm^{-1}: 1726, 1551. $[\alpha]^{24}_D$ −25.0 (*c* 0.106, EtOH).

Methyl (3*S*,4*R*)-4-(2.6-Difluoro-4-methoxyphenyl)-2-oxopyrrolidine-3-carboxylate (43). Compound **43** (10.5 g, 55%) was prepared from **42** (23.3 g, 67.0 mmol) by the same method as that used for **38**. White solid. ^1H NMR ($CDCl_3$) δ: 3.51 (t, J = 9.2 Hz, 1H), 3.67 (dt, J = 9.2, 1.2 Hz, 1H), 3.78−3.81 (m, 7H), 4.46 (q, J = 9.2 Hz, 1H), 6.24 (br, 1H), 6.47 (d, J = 10.4 Hz, 2H). MS (ESI^+) *m/z*: 286 ($M^+ + H$). HRMS (ESI^+) for $C_{13}H_{14}F_2NO_4$ ($M^+ + H$): calcd, 286.08909; found, 286.08922. IR (ATR) cm^{-1}: 3219, 1742, 1706. $[\alpha]^{24}_D$ −120 (*c* 0.106, EtOH).

(3*S*,4*R*)-4-(2,6-Difluoro-4-methoxyphenyl)-2-oxopyrrolidine-3-carboxylic Acid (44). Compound **44** (9.85 g, 100%) was prepared from **43** (10.4 g, 36.4 mmol) by the same method as that used for **39**. White solid. ^1H NMR (DMSO−d_6) δ: 3.25 (t, J = 9.2 Hz, 1H), 3.43 (d, J = 10.4 Hz, 1H), 3.56 (t, J = 9.2 Hz, 1H), 3.76 (s, 3H), 4.14 (q, J = 9.2 Hz, 1H), 6.73−6.79 (m, 2H), 8.20 (s, 1H), 12.8 (br, 1H). MS (ESI^+) *m/z*: 272 ($M^+ + H$). HRMS (ESI^+) for $C_{12}H_{12}F_2NO_4$ ($M^+ + H$): calcd, 272.07344; found, 272.07428. IR (ATR) cm^{-1}: 3263, 1726, 1638. $[\alpha]^{23}_D$ −121 (*c* 0.100, EtOH).

Benzyl [(3*S*,4*R*)-4-(2,6-difluoro-4-methoxyphenyl)-2-oxopyrrolidin-3-yl]carbamate (45). To a solution of **44** (3.00 g, 11.1 mmol) in toluene (157 mL) and MeCN (42 mL) were added triethylamine (1.70 mL, 12.2 mmol) and diphenylphosphoryl azide (3.00 mL, 13.4 mmol), and the mixture was stirred at room temperature for 2 h. Benzyl alcohol (5.70 mL, 55.1 mmol) was added to the reaction mixture, and the mixture was stirred at 80 °C for 30 min and then 110 °C for 2 h. After removal of MeCN in vacuo, the resulting mixture was washed with water and brine, dried over anhydrous Na_2SO_4, filtered, and concentrated in vacuo. A mixture of the residue and benzyl alcohol (11.3 mL, 109 mmol) was stirred at 110 °C for 23 h. Flash chromatography (hexane/AcOEt = 4:1 → 1:1 → AcOEt) of the resulting mixture gave **45** (1.93 g, 47%). ^{1}H NMR ($CDCl_3$) δ: 3.48−3.62 (m, 2H), 3.79 (s, 3H), 3.80−3.96 (m, 1H), 4.67−4.75 (m, 1H), 5.05 (s, 2H), 5.37 (br d, 1H), 6.46 (br d, 2H), 6.60 (s, 1H), 7.26−7.36 (m, 5H). MS (ESI$^+$) *m/z*: 377 (M^+ + H). HRMS (ESI$^+$) for $C_{19}H_{19}F_2N_2O_4$ (M^+ + H): calcd, 377.13129; found, 377.13184. $[\alpha]^{24}_D$ −107 (*c* 0.102, EtOH).

(3*S*,4*R*)-3-Amino-4-(2,6-difluoro-4-methoxyphenyl)pyrrolidin-2-one (46). A suspension of **45** (811 mg, 2.15 mmol) and 10% Pd−C (wetted with ca. 55% water, 81.0 mg) in EtOH (30 mL) was stirred at room temperature for 2 h under H_2 atmosphere. After the insoluble materials were filtered off, the filtrate was concentrated in vacuo. Flash chromatography (hexane/AcOEt = 1:1 → AcOEt → AcOEt/MeOH = 5:1) of the residue gave **46** (525 mg, 100%). ^{1}H NMR (DMSO−d_6) δ: 1.78 (br s, 2H), 3.22 (t, J = 8.6 Hz, 1H), 3.34−3.48 (m, 3H), 3.76 (s, 3H), 6.74 (d, J = 11.0 Hz, 2H), 7.88 (br s, 1H). MS (ESI$^+$) *m/z*: 243 (M^+ + H). HRMS (ESI$^+$) for $C_{11}H_{13}F_2N_2O_2$ (M^+ + H): calcd, 243.09451; found, 243.09492. $[\alpha]^{24}_D$ −90.1 (*c* 0.110, EtOH).

1-[(3*S*,4*R*)-4-(2,6-Difluoro-4-methoxyphenyl)-2-oxopyrrolidin-3-yl]-3-(4-fluorophenyl)urea (12g). To a mixture of **44** (3.00 g, 11.1 mmol), toluene (110 mL) and MeCN (30 mL) was added triethylamine (1.69 mL, 12.2 mmol) and diphenyphosphoryl azide (2.72 mL, 12.2 mmol), and the mixture was stirred at room temperature for 1 h and then at 80 °C for 30 min. To the reaction mixture was added 4-fluoroaniline (2.11 mL, 22.0 mmol), and the mixture was stirred at 110 °C for 2 h. After cooling to room temperature, the reaction mixture was concentrated in vacuo. To the residue was added 1 M HCl, and the mixture was extracted with AcOEt. The extract was washed with water and brine, dried over anhydrous Na_2SO_4, filtered, and concentrated in vacuo. Flash chromatography (hexane/AcOEt = 1:1 → AcOEt → AcOEt/MeOH = 95:5) of the residue gave **12g** (2.29 g, 55%) as a white powder. Mp: 194−197 ℃ ^{1}H NMR (DMSO−d_6) δ: 3.31 (t, J = 9.7 Hz, 1H), 3.45 (t, J = 9.1 Hz, 1H), 3.76 (s, 3H), 3.80 (q, J = 10.9 Hz, 1H), 4.58 (dd, J = 10.9 8.5 Hz, 1H), 6.47 (d, J = 7.9 Hz, 1H), 6.75 (d, J = 10.3 Hz, 2H), 6.99−7.06 (m, 2H), 7.31−7.37 (m, 2H), 8.07 (s, 1H), 8.68 (s, 1H). MS (ESI$^+$) *m/z*: 380 (M^+ + H). HRMS (ESI$^+$) for $C_{18}H_{17}F_3N_3O_3$ (M^+ + H): calcd, 380.12220; found, 380.12171. IR (ATR) cm^{-1}: 3316, 1711, 1638. $[\alpha]^{28}_D$ −156 (*c* 0.101, EtOH). HPLC purity 99.4%.

1-[(3*S*,4*R*)-4-(2,6-Difluoro-4-methoxyphenyl)-2-oxopyrrolidin-3-yl]-3-phenylurea (13c). A mixture of **46** (74.3 mg, 0.306 mmol) and phenyl isocyanate (33.0 μL, 0.306 mmol) in THF (3.1 mL) was stirred at room temperature for 15 min, and concentrated in vacuo. Flash chromatography (hexane/AcOEt = 4:1 → AcOEt) of the residue gave **13c** (83.8 mg, 76%) as a white powder. Mp: 211−213 ℃. ^{1}H NMR (DMSO−d_6) δ: 3.31 (t, J = 9.1 Hz 1H), 3.46 (t, J = 9.1 Hz, 1H), 3.76 (s, 3H), 3.80 (q, J = 9.1 Hz, 1H), 4.58 (dd, J = 10.9, 8.5 Hz, 1H), 6.47 (d, J = 8.5 Hz, 1H), 6.75 (d, J = 10.9 Hz, 2H), 6.85−6.89 (m, 1H), 7.16−7.27 (m, 2H), 7.31−7.35 (m, 2H), 8.07 (s, 1H), 8.63 (s, 1H). MS (ESI$^+$) *m/z*: 362 (M^+ + H). HRMS (ESI$^+$) for $C_{18}H_{18}F_2N_3O_3$ (M^+ + H): calcd, 362.13162;

found, 362.13145. IR (ATR) cm^{-1}: 3315, 1709, 1638. $[\alpha]^{27}_D$ −162 (*c* 0.103, EtOH). HPLC purity 98.1%.

1-[(3*S*,4*R*)-4-(2,6-difluoro-4-methoxyphenyl)-2-oxopyrrolidin-3-yl]-3-(3,4-difluorophenyl)urea (13i). Compound **13i** (56.6 mg, 86%) was prepared from **46** (40.0 mg, 0.165 mmol) and 3,4-difluorophenyl isocyanate (20.0 μL, 0.165 mmol) by the same method as that used for **13c**. White amorphous solid. ^{1}H NMR (DMSO−d_6) δ: 3.31 (t, J = 9.7 Hz, 1H), 3.46 (t, J = 9.1 Hz, 1H), 3.76 (s, 3H), 3.82 (q, J = 9.7 Hz, 1H), 4.57 (dd, J = 10.9, 8.5 Hz, 1H), 6.59 (d, J = 8.5 Hz, 1H), 6.75 (d, J = 10.9 Hz, 2H), 6.99−7.04 (m, 1H), 7.22−7.29 (m, 1H), 7.54 (ddd, J = 10.3, 7.9, 3.0 Hz, 1H), 8.08 (s, 1H), 8.90 (s, 1H). MS (ESI$^+$) *m/z*: 398 (M^+ + H). HRMS (ESI$^+$) for $C_{18}H_{16}F_4N_3O_3$ (M^+ + H): calcd, 398.11278; found, 398.11214. IR (ATR) cm^{-1}: 3303, 1666, 1638. $[\alpha]^{27}_D$ −138 (*c* 0.100, EtOH). HPLC purity 99.5%.

1-[(3*S*,4*R*)-4-(2,6-Difluoro-4-methoxyphenyl)-2-oxopyrrolidin-3-yl]-3-(3-hydroxy-4-methylphenyl)urea (13l). Compound **13l** (105 mg, 65%) was prepared from **44** (130 mg, 0.387 mmol) and 5-amino-2-methylphenol (95.0 mg, 0.771 mmol) by the same method as that used for **12g**. White amorphous solid. ^{1}H NMR (DMSO−d_6) δ: 1.99 (s, 3H), 3.30 (t, J = 9.7 Hz, 1H), 3.45 (t, J = 9.7 Hz, 1H), 3.72−3.80 (m, 4H), 4.58 (dd, J = 10.9, 8.5 Hz, 1H), 6.32 (d, J = 8.5 Hz, 1H), 6.56 (dd, J = 7.9, 2.4 Hz, 1H), 6.74 (d, J = 10.9 Hz, 2H), 6.83 (d, J = 8.5 Hz, 1H), 6.99 (d, J = 2.4 Hz, 1H), 8.07 (s, 1H), 8.41 (s, 1H), 9.10 (s, 1H). MS (ESI$^+$) *m/z*: 392 (M^+ + H). HRMS (ESI$^+$) for $C_{19}H_{20}F_2N_3O_4$ (M^+ + H): calcd, 392.14219; found, 392.14299. IR (ATR) cm^{-1}: 3302, 1638. $[\alpha]^{25}_D$ −151 (*c* 0.151, EtOH). HPLC purity 97.9%.

1-(5-Chlorothiophen-2-yl)-3-[(3*S*,4*R*)-4-(2,6-difluoro-4-methoxyphenyl)-2-oxopyrrolidin-3-yl]urea (13n). To a mixture of 2-chlorothiophene-5-carboxylic acid (60.0 mg, 0.369 mmol), triethylamine (51.0 μL, 0.369 mmol) in toluene (3.7 mL) was added diphenylphosphoryl azide

(83.0 μL, 0.369 mmol), and the mixture was stirred at 40 °C for 1 h, 50 °C for 1 h, and then at 100 °C for 1 h. After addition of **46** (44.8 mg, 0.185 mmol), the mixture was stirred at 100 °C for 15 min. After addition of **46** (26.6 mg, 0.110 mmol), the mixture was stirred at 100 °C for 3 h, and concentrated in vacuo. Flash chromatography (hexane/AcOEt = 3:1 → AcOEt) of the residue gave **13n** (45.0 mg, 38%) as a white powder. Mp: 180−183 °C. ^{1}H NMR (DMSO−d_6) δ: 3.31 (t, J = 9.7 Hz, 1H), 3.46 (t, J = 9.1 Hz, 1H), 3.76 (s, 3H), 3.86 (q, J = 9.7 Hz, 1H), 4.54 (dd, J = 10.9, 8.5 Hz, 1H), 6.22 (d, J = 4.2 Hz, 1H), 6.72−6.79 (m, 4H), 8.08 (s, 1H), 9.95 (s, 1H). MS (ESI$^+$) *m/z*: 402 (M^+ + H). HRMS (ESI$^+$) for $C_{16}H_{15}ClF_2N_3O_3S$ (M^+ + H): calcd, 402.04907; found, 402.04877. IR (ATR) cm^{-1}: 3275, 1713, 1664, 1638. $[\alpha]^{27}_D$ −135 (*c* 0.105, EtOH). HPLC purity 99.8%.

Pharmacology and Biology

Animal studies were carried out in accordance with American Association for Accreditation of Laboratory Animal Care guidelines and protocols were approved by Bristol-Myers Squibb and University of California San Diego Animal Care and Use committees.

Calcium Mobilization Assays. HEK293 cells were obtained from NIHS (JCRB; Cell number JCRB9068) and maintained in Dulbecco's Modified Eagle Medium (Thermo Fisher Scientific, Waltham, MA) supplemented with 10% heat-inactivated fetal bovine

serum and 100 U/mL penicillin/streptomycin at 37°C under 5% CO_2. HEK293 cells were transfected with plasmids encoding human FPR1, human FPR2, or mouse FPR2 together with Gα15 using Lipofectamine 2000 reagent (Invitrogen) according to the manufacturer's protocol. After 24 h incubation, the HEK293 cells expressing FPRs/Gα15 were re-seeded in Biocoat Poly-D-Lysine 96-well plates (7 x 10^4 cells/well) and further incubated for an additional day. Changes in intracellular Ca^{2+} were measured with a FlexStation III scanning fluorometer (Molecular Devices Co., Ltd.) using a Fluo-4 NW Calcium Assay Kit (Invitrogen). Briefly, cell culture medium was replaced to dye loading solution (90 μL/well) and incubated for 45 min at 37°C under 5% CO_2. After removing dye loading solution, 90 μL/well of assay buffer was added to each well, and plates were mounted in the FlexStation III. The fluorescence intensity (Excitation at 485 nm, and Emission at 525 nm) was measured for 80 sec at 1.5 sec interval after adding the assay solutions including test compounds (10 μL/well) to cells. The value was quantified as the maximal peak height, which was calculated automatically by subtracting the basal value from the maximal value during each measurement. Curve fitting and calculation of EC_{50} were performed by nonlinear regression analysis of the dose–response curves generated using

Prism 4 (GraphPad Software, Inc., San Diego, CA). Compound 43 (Figure 1) was used as an internal standard: hFPR2 EC_{50} = 8.4 nM (SD = 7.4, n = 173), hFPR1 EC_{50} = 9.0 nM (SD = 7.1, n = 75).

FPR2 and FPR1 Cyclic Adenosine Monophosphate (cAMP) Assays. A mixture of forskolin (5 μM final for FPR2 or 10 μM final for FPR1) and IBMX (200 μM final) were added to 384-well Proxiplates (Perkin-Elmer) pre-dotted with test compounds in DMSO (1% final) at final concentrations in the range of 1.7 nM to 100 μM. Chinese Hamster Ovary cells (CHO) overexpressing human FPR1 or human FPR2 receptors were cultured in F-12 (Ham's) medium supplemented with 10% qualified FBS, 250 μg/ml zeocin and 300 μg/ml hygromycin (Life Technologies). Reactions were initiated by adding 2,000 human FPR2 cells per well or 4,000 human FPR1 cells per well in Dulbecco's PBS (with calcium and magnesium) (Life Technologies) supplemented with 0.1% BSA (Perkin-Elmer). The reaction mixtures were incubated for 30 min at room temperature. The level of intracellular cAMP was determined using the HTRF HiRange cAMP assay reagent kit (Cisbio) according to manufacturer's instruction. Solutions of cryptate conjugated anti-cAMP and d2 flurorophore-labelled cAMP were made in a supplied lysis buffer separately.

Upon completion of the reaction, the cells were lysed with equal volume of the d2-cAMP solution and anti-cAMP solution. After a 1-h room temperature incubation, time-resolved fluorescence intensity was measured using the Envision (Perkin-Elmer) at 400 nm excitation and dual emission at 590 nm and 665 nm. A calibration curve was constructed with an external cAMP standard at concentrations ranging from 1 μM to 0.1 pM by plotting the fluorescent intensity ratio from 665 nm emission to the intensity from the 590 nm emission against cAMP concentrations. The potency and activity of a compound to inhibit cAMP production was then determined by fitting to a 4-parametric logistic equation from a plot of cAMP level versus compound concentrations Values are an average of at least 2 test occasions.

Chemotaxis Assay. HL-60 cells were differentiated for 5 days in 1.2% DMSO. Assay media was phenol red free RPMI with 0.2% fatty acid free BSA. Approximately $1X10^6$ cells were added to the upper chamber of a transwell-plate (Corning#3387). Migration was induced by placing chemoattractant in the bottom chamber and the dHL-60 cells in the top chamber. Following migration, dHL-60 cells in the lower chamber (migrated fraction) were quantitated using a luminescence cell viability assay (Promega, G7571).

Phagocytosis. Mice were injected i.p. with 1ml of 2% BioGel P100 solution (BioRad, Inc.). After 4 days, the peritoneum was lavaged with PBS/2mM EDTA. Residual BioGel particles were removed by passing the exudate through a 40 μm strainer. Cells were washed with PBS and then seeded into 96-well plates (Costar 3904) at a density of $1.2x10^5$ cells/well. After 90min, non-adherent cells were removed by washing with PBS and the macrophages were incubated overnight in Macrophage-SFM media (ThermoFisher, Inc.). Macrophages were treated with test compound for 15 minutes and then fed opsonized FITC labeled zymosan (1:8 ratio of cells:zymosan) for 45 min at 37°C. Cells were washed and extracellular fluorescence was quenched with 0.025% Trypan Blue. Phagocytosis was measured using a SpectraMAX Gemini EM plate reader (Molecular Devices, Inc.).

Pharmacokinetic study in animals. Male mice (BALB/cCrSlc for oral administration, Crl:CD1(ICR) for intravenous administration), male rats (Crl:CD(SD)), male dogs (beagle), and male monkeys (cynomolgus) were used. The **13c** suspensions in 0.5% MC were orally administered. The **13c** solution in DMSO/PEG400/saline (5/47.5/47.5) was

administered from the vein. The blood was collected to a micro haematocrit capillary tube (EDTA 2K). After the centrifugation, the plasma samples were stored in a freezer until analysis. The plasma samples were mixed with methanol/acetonitrile (1:1) and the internal standard solution. After the centrifugation, the supernatant was mixed with purified water. The concentration of **13c** was determined by a liquid chromatography tandem mass spectrometry (LC-MS/MS) method.

The area under plasma concentration curve from 0 to infinity was calculated using trapezoidal rule. Extrapolation to infinity was accomplished using the elimination rate constant (k_{el}) calculated from the terminal phase of the plasma concentration-time curve. The half-life ($t_{1/2}$) was calculated as ln2 / k_{el}. The bioavailability (BA) was determined using the equation of BA = ($AUC_{0\text{-inf, p.o.}}$ / dose, $_{p.o.}$) / ($AUC_{0\text{-inf, i.v.}}$ / dose, $_{i.v.}$) × 100.

Metabolic stability of 13c in human and animal liver microsomes. The suspension of liver microsomes with NADPH regenerating systems was pre-incubated at 37°C for 5 min. By adding **13c** standard solution, the metabolic reaction was initiated. Final concentrations of **13c** and microsomal protein were 0.1 μmol/L and 1 mg protein/mL, respectively. After the incubation at 37°C for 0, 2, 5, 10, 15, 20, 30 and 60 min, an aliquot

of the reaction mixture was mixed with methanol/acetonitrile (1/1) and the internal standard solution, followed by the centrifugation. The supernatant was diluted with purified water. An aliquot of the diluted supernatant was injected into the LC-MS/MS system to determine **13c** concentration. All procedures were run in triplicate. The elimination rate constant (k_{el}) was calculated from the residual ratio–time curve using five time points from 5 min to 30 min. Intrinsic hepatic clearance ($CL_{int,\ in\ vitro}$) was calculated using the equation of $CL_{int,\ in\ vitro}$ (mL/min/mg protein) = k_{el} (min^{-1}) / microsomal protein concentration (mg protein/mL).

Metabolic stability of 13c in human and animal hepatocytes. The suspension of hepatocytes (1×10^6 cells/mL) in Krebs–Henseleit Buffer Modified was pre-incubated at 37°C for 5 min. By adding **13c** standard solution to the mixture and mixing gently, the metabolic reaction was initiated. Final concentration of **13c** was 0.1 μmol/L. After the incubation at 37°C for 0, 1, 2, 4 and 6 h, an aliquot of the reaction mixture was mixed with methanol/acetonitrile (1/1), followed by the centrifugation. The supernatant was mixed with internal standard solution and purified water. An aliquot of the mixture was injected

into the LC-MS/MS system to determine **13c** concentration. All procedures were run in duplicate.

The elimination rate constant (k_{el}) was calculated from the residual ratio–time curve using three time points from 0 to 2 h. Intrinsic hepatic clearance ($CL_{int,\ in\ vitro}$) was calculated using the equation of $CL_{int,\ in\ vitro}$ (mL/min/kg) = k_{el} (h^{-1}) / 60 / (hepatocytes concentration (cells/mL) / hepatocellularity numbers (cells/g liver) / liver weight (g liver/kg)).

Mouse Myocardial Infarction Studies. Male C57BL/6 mice were purchased from the Jackson Laboratory and were 10-12 weeks of age at the time of surgery. Myocardial infarction was induced by permanent ligation of the left anterior descending coronary artery (LAD) using two procedures. For 28-day studies mice were anesthetized with a mixture of ketamine (100mg/kg) and xylazine (8mg/kg) given via the intraperitoneal route followed by oral intubation with a modified endotracheal tube. Mice were placed in a right lateral position on a circulating-water heating pad for maintenance of normal body temperature and mechanically ventilated at a tidal volume of ~ 0.5ml and ~105 respirations per min. The neck and chest areas were shaved and prepped with a 70%

isopropyl alcohol followed by betadine solution. Following draping for aseptic surgery the heart was exposed via a left thoracotomy in the fourth intercostal space, and the pericardium incised. The descending left coronary artery was regionally located (*ramus interventricularis paraconalis*). Animals were randomized into treatment groups. The coronary artery was permanently ligated with a silk suture with a tapered curved 6mm needle. Complete coronary occlusion was confirmed visually by noting the prompt and sustained pallor of the anterior wall distal to the ligation site. For animals designated as Sham, the snare was placed but not tightened. The chest was closed in layers and the pneumothorax evacuated. For pain management a local anesthetic (bupivacaine) was infiltrated subcutaneously along the edges of the incision sites, and buprenorphine (0.05-0.1 mg/kg) administered immediately post-operatively. Animals were returned to their cage, given water and standard rodent chow ad libitum, and monitored daily until the terminal procedure. Mice were dosed daily (QD) with compound **13c**, captopril or with vehicle for 28 days. Dosing was initiated 24 h post MI. Dosing route with compound **13c** and vehicle was oral (PO) via gavage at a dose volume of 5ml/kg. Treatment with the

angiotensin converting enzyme inhibitor captopril was provided in the drinking water (~ 100 mg/kg/day).

Ex Vivo Passive Mechanics. Following exposure of the heart via thoracotomy, the heart was arrested in diastole by rapid intracardiac infusion of ice-cold cardioplegic solution containing high potassium and 2,3 butanedione monoxime. The heart was excised, the aorta cannulated and the heart perfused with cardioplegia to flush out residual blood. The atrial appendages were trimmed, the hearts weighed and a cardiac balloon inserted into the left ventricle (LV) across the mitral valve. The hearts were mounted onto a pressure-volume (PV) measurement stand and multiple epicardial surface markers placed onto the anterior wall. A digital camera was positioned to enable capture of video images of the anterior surface of the heart. PV curves were obtained by digitally acquiring left ventricular pressure and volume during balloon inflations. There were 2 to 3 conditioning runs followed by 2 to 3 data acquisition runs with maximal LV pressure of ~50mmHg. Synchronized video images were obtained during each data run. Following acquisition of the PV data, the hearts were perfusion-fixed for 5 to 10 minutes by infusion of 10%

formalin into the aortic cannula while maintaining LV balloon pressure at 10 to 15 mm Hg. Hearts were stored in 10% formalin at room temperature for subsequent histologic processing

ASSOCIATED CONTENT

Supporting Information. The following files are available free of charge.

Experimental procedures for compounds **2a–d**, **12a–f,h–l**, **13a,b,d–h,j,k,m,o–q** (PDF),

Molecular Formula Strings for all compound included in the article.

AUTHOR INFORMATION

Corresponding Authors

* YA: E-mail: yoshikazu.asahina@mb.kyorin-pharm.co.jp; NRW: Phone: 609-466-5099. E-mail: nicholas.wurtz@bms.com

ORCHID

Nicholas Wurtz: 0000-0003-2574-9440

Yoshikazu Asahina: 0000-00020668-800X

Author Contributions

The manuscript was written through contributions of all authors. All authors have given approval to the final version of the manuscript.

ABBREVIATIONS USED

ACEi, angiotensin-converting enzyme inhibitor; BALF, Bronchoalveolar lavage fluid; cAMP, Cyclic adenosine monophosphate; CHO, Chinese hamster ovary; CL, Clearance; CYP, cytochrome P; DPPA, Diphenyl Phosphorylazide; fMLP aka fMPF, *N*-formyl-methionyl-leucyl-phenylalanine; FPR, formyl peptide receptor; IL, interleukin; LAD, left anterior descending artery; LV, left ventricle; MI, myocardial infarction; P-V, pressure volume; SAA, serum amyloid A

REFERENCES

(1) Ye, R. D.; Boulay, F.; Wang, J. M.; Dahlgren, C.; Gerard, C.; Parmentier, M.; Serhan, C, N.; Murphy, P. M. International union of basic and clinical pharmacology. LXXIII. Nomenclature for the formyl peptide receptor (FPR) family. *Pharmacol*. *Rev*. **2009**, *61*, 119−161.

(2) Bao, L.; Gerard, N. P.; Eddy Jr., R. L.; Shows, T. B.; Gerard, C. Mapping of genes for the human C5a receptor (C5AR), human FMLP receptor (FPR), and two FMLP receptor homologue orphan receptors (FPRH1, FPRH2) to chromosome 19. *Genomics* **1992**, *13*, 437−440.

(3) Le, Y.; Murphy, P. M.; Wang, J. M. Formyl-peptide receptors revisited. *Trends Immunol*. **2002**, *23*, 541−548.

(4) Yang, S. C.; Hwang, T. L. The potential impacts of formylpeptide receptor 1 in inflammatory diseases. *Front*. *Biosci*., *Elite Ed*. **2016**, *8*, 436−449.

(5) He, R.; Sang, H.; Ye, R. D. Serum amyloid A induced IL-8 secretion through a G protein-coupled receptor, FPRL1/LXA4R. *Blood* **2003**, *101*, 1572−1581.

(6) Chiang, N.; Serhan, C. N.; Dahlén, S-E.; Drazen, J. M.; Hay, D. W. P.; Rovati, G. E.; Shimizu, T.: Yokomizo, T.; Brink, C. The lipoxin receptor ALX: Potent ligand-specific and stereoselective actions in vivo. *Pharmacol*. *Rev*. **2006**, *58*, 463−489.

(7) Perretti, M.; Chiang, N.; La, M.; Fierro, I. M.; Marullo, S.; Getting, S. J.; Solito, E.; Serhan, C. N. Endogenous lipid- and peptide derived anti-inflammatory pathways generated with glucocorticoid and aspirin treatment activate the lipoxin A4 receptor. *Nat*. *Med*. **2002**, *8*, 1296−1302.

(8) Bena, S.; Brancaleone, V.; Wang, J. M.; Perretti, J. M.; Flower, R. J. Annexin A1 interaction with the FPR2/ALX receptor. *J*. *Biol*. *Chem*. **2012**, *287*, 24690−24697.

(9) Cattaneo, F.; Parisi, M.; Ammendola, R. Distinct signaling cascades elicited by different formyl peptide receptor 2 (FPR2) agonists. *Int*. *J*. *Mol*. *Sci*. **2013**, *14*, 7193−7230.

(10) Nash, N.; Scully, A.; Gardeli, L.; Olsson, R.; Gustafsson, M. Use of the Lipoxin Receptor, FPRL1, as a Tool for Identifying Compounds Effective in the Treatment of Pain and Onflammation. PCT Int. Appl. WO 2005/047899, 2005.

(11) Schepetkin, I. A.; Khlebnikov, A. I.; Giovannoni, M. P.; Kirpotina, L. N.; Cilibrizzi, A.; Quinn, M. T. Development of small molecule non-peptide formyl peptide receptor (FPR) ligands and molecular modeling of their recognition. *Curr*. *Med*. *Chem*. **2014**, *21*, 1478−1504.

(12) Corminboeuf, O.; Leroy, X. FPR2/ALXR agonists and the resolution of inflammation. *J*. *Med*. *Chem*. **2015**, *58*, 537−559.

(13) Tsai, Y-F.; Yang, S-C.; Hwang, T-L. Formyl peptide receptor modulators: a patent review and potential applications for inflammatory diseases (2012-2015). *Expert Opin*. *Ther*. *Pat*.

2016, *26*, 1139−1156.

(14) Schepetkin, I. A.; Khlebnikov, A. I.; Kirpotina, L. N.; Quinn, M. T. Antagonism of human formyl peptide receptor 1 with natural compounds and their synthetic derivatives. *Int. Immunopharmacol*. **2016**, *37*, 43−58.

(15) Bürli, R. W.; Xu, H.; Zou, X.; Muller, L.; Golden, J.; Frohn, M.; Adlam, M.; Plant, M. H.; Wong, M.; McElvain, M.; Regal, K.; Viswanadhan, V. N.; Tagari, P.; Hungate, R. Potent hFPRL1 (ALXR) agonists as potential anti-inflammatory agents. *Bioorg. Med. Chem. Lett.* **2006**, *16*, 3713−3718.

(16) García, R.; Ito, B.; Lupisella, J,; Carson, N.; Hsu, M.; Fernando, G.; Heroux, M.; Bouvier, M.; Dierks, E.; Kick, E.; Gordon, D.; Chen, J.; Mintier, G.; Carrier, M.; Onge, S.; Shah, H.; Towne, J.; Bucardo, M.; Ma X.; Ryan, C.; Wurtz, N.; Ostrowski, J.; Villarreal, F. Preservation of post-infarction cardiac structure and function via long-term oral formyl peptide receptor agonist treatment. *J. Am. Coll. Cardiol. Basic Trans. Science* **2019**, *4*, 905-920.

(17) Frohn, M.; Xu, H.; Zou, X.; Chang, C.; McElvain, M.; Plant, M. H.; Wong. M.; Tagari, P.; Hungate, R.; Bürli, R. W. New 'chemical probes' to examine the role of the hFPRL1 (or ALXR) receptor in inflammation. *Bioorg. Med. Chem. Lett.* **2007**, *17*, 6633−6637.

(18) Corminboeuf, O.; Cren, S. 1-(p-Tolyl)cyclopropyl Substituted Bridged Spiro[2.4]heptane Derivatives as ALX Receptor Agonists. PCT Int. Appl. WO 2013/171687, 2013.

(19) Bur, D.; Corminboeuf, O.; Cren, S.; Grisostomi, C.; Leroy, X.; Richard-Bikdstein S. Fluorinated Aminotriazole Derivatives. PCT Int. Appl. WO2010/143116, 2010.

(20) Qin, C. X.; May, L. T.; Li, R.; Cao, N.; Rosli, S.; Deo, M.; Alexander, A. E.; Horlock, D.; Bourke, J. E.; Yang, Y. H.; Stewart, A. G.; Kaye, D, M.; Du, X-J.; Sexton, P. M.; Christopoulos, A.; Gao, X-M.; Ritchie, R. H. Small-molecule-biased formyl peptide receptor agonist

compound 17b protects agonist myocardial ischaemia-reperfusion injury in mice. *Nat. Commun*. **2017**, *8*, 14232.

(21) Stalder, A. K.; Lott, D.; Strasser, D. S.; Cruz, H. G.; Krause, A.; Groenen, P. M. A.; Dingemanse, J. Biomarker-guided clinical development of the first-in-class anti-inflammatory FPR2/ALX agonist ACT-389949. *Br. J. Clin. Parmacol*. **2017**, *83*, 476−486.

(22) Kirpotina, L. N.; Khlebnikov, A. I.; Schepetkin, I. A.; Ye, R. D.; Rabiet, M-J.; Jutila, M. A.; Quinn, M. T. identification of novel small-molecule agonists for human formyl peptide receptors and pharmacophore models of their recognition. *Mol. Pharmacol*. **2010**, *77*, 159−170.

(23) (a) Zarei, M. A straightforward approach to 2-azetidinones from imines and carboxylic acids using dimethylsulfoxide and acetic anhydride. *Tetrahedron Lett*. **2014**. *55*, 5354−5357. (b) Zarei, M. β-Lactam preparation via Staudinger reaction with activated dimethylsulfoxide. *J. Hetrocycl. Chem.* **2017**, *54*, 1161−1166.

(24) Guo, M.; Min, J.; Li, R; Zhang, L. Studies on monocyclic β-lactams. (I). Synthesis of 3-hydroxy-4-substituted-2-azetidinones. *Gaodeng Xuexiao Huaxue Xuebao* **1992**, *13*, 919−922.

(25) Li, B.; Wang, Y.; Du, D-M.; Xu, J. Notable and obvious ketene substituent-dependent effect pf temperature on the stereoselectivity in the Staudinger reaction. *J. Org. Chem*. **2007**, *72*, 990−997.

(26) Gairaud, C.; Lappin, G. R. The synthesis of ω-nitrostyrenes. *J. Org. Chem*. **1953**, *18*, 1−3.

(27) Yamada, K.; Kishikawa, K.; Yamamoto, M. Stereospecificity of the photorearrangement of nitronate anions and its utilization for stereospecific cleavage of cyclic compounds. *J. Org. Chem*. **1987**, *52*, 2327−2330.

(28) Ronsen B.; Upadiyaya, S. P. Process for Preparing Arylpiperidine Carbinol Intermediates

and Derivatives. PCT Int. Appl. WO2000/037443, 2000.

(29) (a) Evans, D. A.; Mito, S.; Seidel, D. Scope and mechanism of enantioselective Michael additions of 1,3-dicarbonyl compounds to nitroalkenes catalyzed by nickel(II)-diamine complexes. *J. Am. Chem. Soc.* **2007**, *129*, 11583−11592. (b) Okino, T.; Hoashi, Y.; Furukawa, T.; Xu, X.; Takemoto, Y. Enantio- and diastereoselective Michael reaction of 1,3-dicarbonyl compounds to nitroolefins catalyzed by a bifunctional thiourea. *J. Am. Chem. Soc.* **2005**, *127*, 119−125. (c) Li, H.; Wang, Y.; Tang, L.; Deng, L. Highly enantioselective conjugate addition of malonate and β-ketoester to nitroalkenes: Asymmetric C−C bond formation with new bifunctional organic catalysts based on cinchona alkaloids. *J. Am. Chem. Soc.* **2004**, *126*, 9906−9907.

(30) Hynes, P. S.; Stupple, P. A.; Dixon, D. J. Organocatalytic asymmetric total synthesis of (R)-Rolipram and formal synthesis of (3S,4R)-Paroxetine. *Org. Lett.* **2008**, *10*, 1389−1391.

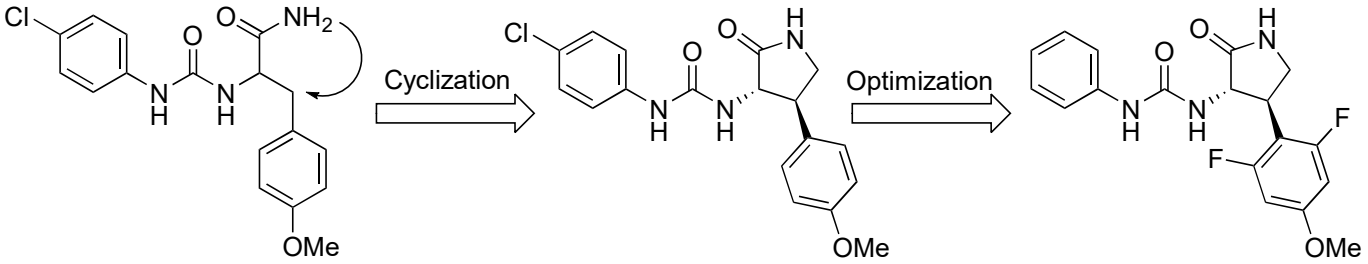

2d
hFPR2 EC_{50}: 4 nM

11a
hFPR2 EC_{50}: 0.9 nM
40x selective over FPR1

13c
hFPR2 EC_{50}: 0.4 nM
7000x selective over FPR1